CHAPTER ONE

INTRODUCTION

1.1 Background

Linear Induction Motor abbreviated as LIM, is basically a special purpose motor that is in use to achieve rectilinear motion rather than rotational motion as in the case of conventional motors. This is quite an engineering marvel, to convert a general motor for a special purpose with more or less similar working principle, thus enhancing its versatility of operation. The history of Linear Induction Motors (LIM) started since 19th century, just a few years later after the discovery of the Rotary Induction Motor (RIM) principle, which is going to serve as the platform to understand the general concepts and operation of LIM's discussed in the sequel.

In general terms, the operation of a RIM is defined by the interaction of two main parts: the stator (or primary) and the rotor (also called secondary). The stator consists on a cylindrical slotted structure formed by a stack of steel laminations [1]. Within the slots of the stator. The poly-phase windings are laid uniformly to produce a rotating sinosoidally distributed magnetic field at a speed depending on the frequency of the network and the number of poles. The relative motion between the rotating magnetic field and the conductors of the rotor, induces a voltage in the rotor producing currents flowing through the conductors which also generates its own magnetic field. The interaction (chasing) of these two magnetic fields will produce an electromagnetic torque that drags the rotor in the same direction of the magnetic fields. From the RIM principle, the operation of the LIM can be explained if one imagines the cylindrical slotted structure and the rotor to cut open and rolled flat causing the magnetic fields to travel in a rectilinear direction instead of rotating. The

primary field now interacts with the secondary (also called secondary sheet) conductor, like an aluminum sheet, and produces a rectilinear force or thrust.

In the conceptual description of the LIM operation one can notice the similarities with the RIM however, contrary to the RIM, the LIM has a beginning (leading edge) and an end (trailing edge) [2]. This characteristic of the LIM produces the so called "end effects" that adversely influences in its operation and are basically a field distortion at the entry and exit of the mobile part which can be the primary or the secondary sheet instead.

In industrial fields, LIM has been used in many applications such as: machine tools, material handling and storage, accelerators and launchers, low and medium trains, sliding doors operation, etc [3, 4]. In general all kinds of applications that need linear displacement require accurate controllability of speed, torque and displacement [5]. In open literature there are several different methods used to analysis LIMs, such as Equivalent Circuit Model (ECM), 1-D and 2-D, electromagnetic field analysis and numerical methods including finite-element and finite-difference methods [6, 7].

1.2 Problem Statement

The problem of this thesis is to develop a reliable simulation model that represents the LIM dynamics and analyze the LIM performance and improve the response regarding speed and torque.

1.3 Objectives

The main objectives of this thesis are to:

1. Analysis LIM dynamic response as an electromechanical system and develop mathematical model for simulation using MATLAB/Simulink

2- Construct Lookup tables to provide basic control to get desired output at steady state and even avoid long transient time and allow quick steady state in starting

3- Implement a control system in terms of the frequency and voltage amplitude.

1.4 Methodology

To achieve the thesis objectives the following methodology is used:

- Develop the equivalent circuit for the LIM**.**
- Derive electrical system differential equations that describes the electrical behavior of the system and the equations that calculate thrust**.**
- Develop electrical system representing the LIM in MATLAB/Simulink and generate stator and rotor currents and the machine thrust.
- Tabulate Lookup table to provide control and get desired output thrust.
- Consider the mechanical system and add it to the model to give output of rotor acceleration speed and position for any input values of Voltage and frequency MATLAB/Simulink model execution and get out puts (A_r, v_r, X_r and thrust).
- Construct Lookup tables to provide primary control fulfilling the criterion of the steady state to be reached in small time (before 2 seconds).
- Use a Proportional-Integral controller to restore the system to the former speed quickly by prober tuning of **P** and **I** gains after disturbing force.

1.5 Thesis Layout

This research consists of five chapters. Chapter one gives a background introduction about the LIM it is operation, characteristic, application and analysis methods. Also states the problem statement, sets the objectives and introduce the methodology.

In chapter two the equivalent circuit for the LIM was developed and after that the electrical system equations were derived till the differential equations that describes the electrical behavior of our system in terms of rotor current and stator current.

In chapter three the electrical system implemented in MATLAB/Simulink as a model to be executed and also all the parameters for our chosen LIM were entered.

In chapter four a disturbing force of value1000 N was subjected to the system and it reduced the speed v_r hence we add a PI controller to restore the system to the former speed quickly by prober tuning of **P** and **I** gains

Another case also examined with disturbing force of1000 N at 2s and then at time 3s a change in the speed reference value to new value applied. Again also the **PI** controller restores the system to the new speed quickly by prober tuning of **P** and **I** gains and results were viewed.

In chapter five results were concluded and discussed and recommendations were stated.

CHAPTER TWO

LINEAR INDUCTION MACHINE FUNDAMENTALS

2.1 LIM Working Principle

A linear electric motor's primary typically consists of a flat magnetic core (generally laminated) with transverse slots which are often straight cut with coils laid into the slots, with each phase giving an alternating polarity and so that the different phases physically overlap Figure 2.1 shows typical 3-phase LIM primary core.

.

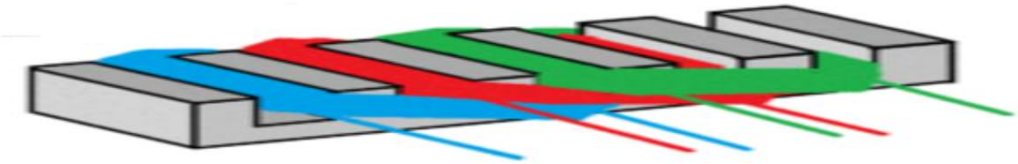

Figure 2.1: Typical 3-phase LIM primary core

The secondary is frequently a sheet of aluminum often with an iron backing plate. Some LIMs are double sided, with one primary either side of the secondary, and in this case no iron backing is needed Figure 2.2 shows LIM side view

.

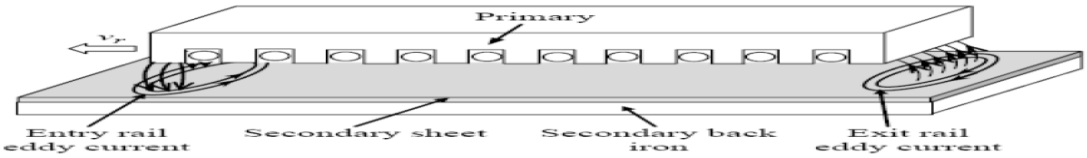

Figure 2.2: Linear Induction Motor LIM side view

Two sorts of linear motor exist, short primary, where the coils are truncated shorter than the secondary, and a short secondary where the conductive plate is smaller. Short secondary LIMs are often wound as parallel connections

between coils of the same phase, whereas short primaries are usually wound in series.

2.2 Performance Model Approach

In need of an equivalent circuit that describes easily and reliably the response of a LIM just like the one used in the per-phase circuit of a rotary induction motor (RIM), A model in which the equivalent circuit of a RIM is modified to account for the "end effects" was proposed and is used to predict the output thrust as well as vertical forces and couples. Before Introducing the equivalent circuit for a LIM a brief description about the "end effects" is going to take place for a better understanding of the system [8]. At the end, as one shall see, the equivalent circuit for a LIM is going to be basically a modification of the equivalent circuit for a rotary induction motor accounting for these effects.

Figure 2.2 shows the end effects as the primary moves to the left, and is feed by 3-phase current which produce a sinusoidal MMF per unit length and a sinusoidal flux density, which are implemented as RMS values, thus accounting as uniform values for the analysis [9]. As the primary moves, new material (in the secondary) enters in the leading edge of the motor where eddy currents rise to their maximum value and also reduce the flux density to zero, but stall growing progressively with a time constant T2 as the eddy currents fade away T2 is defined as follows:

$$T_2 = \frac{(L_m + L_{21})}{R_{21}} \qquad (2.1)$$

L_m: Represents the flux linking the primary and secondary

L_{21} : indicates leakage flux in the secondary, referred to the primary.

R_{21} : Secondary resistance referred to the primary, indicates heating losses in the secondary

T2, also called the total secondary time constant, is the time constant in which eddy currents will decay in the rail after it enters into the primary [10]. On the other hand, Figure 2.2 also illustrates some important facts related to the exit of material (secondary) from the primary. As no MMF from the primary is seen by the rail eddy currents will emerge in it in order to maintain the air gap flux but these will decay very rapidly with a time constant related to the leakage inductance of the rail. The transient and effect of end effects of the motor in shown in Figure 2.3 [11].

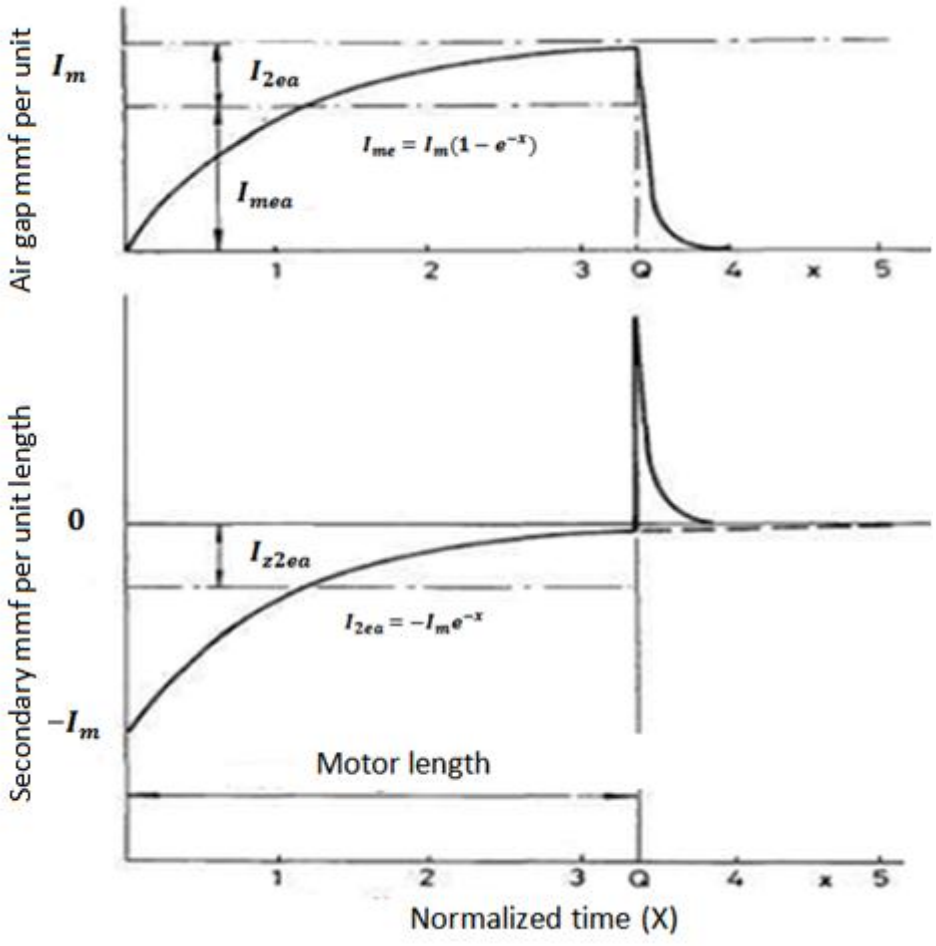

Figure 2.3: Distribution of effective MMF at velocity>0

The ohmic losses due to eddy currents for a resistance $R_{21}$of the circuit is found by Equation (2.2) as follows.

Eddy current losses $= I_m^2 R_{21} \frac{1-e^{-2Q}}{2Q}$ (2.2)

Q: Length of the motor on the normalized scale

I_m: magnetizing branch current

Applying for the section of rail under the primary. As the motor passes the rail over, the MMF seen by the rail disappears and eddy currents will rise in order to maintain the gap flux, as depict in Figure 2.4. The magnetic energy is then dissipated in the ohmic resistance, and the power loss is defined by the following expressions:

Exit power loss $= I_m^2 R_{21} \frac{\{1-e^{-Q}\}^2}{2Q}$ (2.3)

Adding Equation 2.2 and 2.3 the ohmic losses due to eddy currents is:

Total ohmic losses due to eddy current rail $= I_m^2 R_{21} \frac{\{1-e^{-Q}\}}{Q}$ (2.4)

These losses are represented in the equivalent circuit as a resistance in the magnetizing branch dependent on the value of Q:

$R_{21} \frac{\{1-e^{-Q}\}}{Q}$ (2.5)

Thus, accounting for expressions above and according to J. Duncan Figure 2.4 represents the equivalent circuit of a linear induction motor.

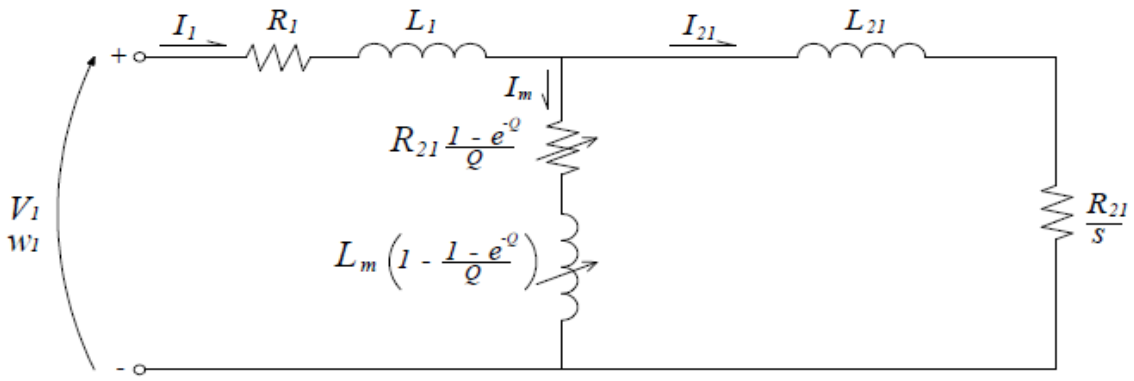

Figure 2.4: Per-phase Equivalent circuit of a Linear Induction Motor

Where:

V_1: Is the phase voltage of the Linear Induction Motor .

R_1: Primary resistance indicates heating losses in the primary coils.

L_1: Indicates leakage flux from the primary, which does not link with secondary

I_1: primary current

I_{21}: secondary current referred to primary

For Double Sided LIM (DSLIM) there is no back iron, it is just the secondary sheet, thus L2 is negligible in DSLIM. The back iron is replaced with another primary however all the relations mentioned previously are applied.

$L_m(1-\frac{\{1-e^{-Q}\}}{Q})$ is a non-linear function that represents the resultant magnetizing flux in the air gap and $R_{21}\frac{\{1-e^{-Q}\}}{Q}$ is Non-linear function that represents the ohmic loss in the secondary due to eddy currents.

The model in Figure 2.4 accounts for the forces and couples generated within a Single Sided Linear Induction Motor (SSLIM) that must be considered in the design of the structure of the motor. The vertical forces can be separated into two components and a turning couple, However in a DSLIM the effects of the vertical forces cancel each other. J. Duncan defines the total thrust of

the motor as the one generated by the slip currents minus the one due to eddy currents.

Motor thrust due to slip currents can be calculated as:

$$3I_{21}^2 R_{21} \frac{\pi}{\omega_2 \tau} \text{ N} \tag{2.6}$$

Motor thrust due to eddy currents can be calculated as:

$$3I_{21}^2 R_{21} \frac{1-e^{-q}}{v\,Q} \text{ N} \tag{2.7}$$

Where:

τ is Motor pole pitch and ω_2 is slip frequency. Figure 2.5 shows Vertical forces and thrust on a DSLIM

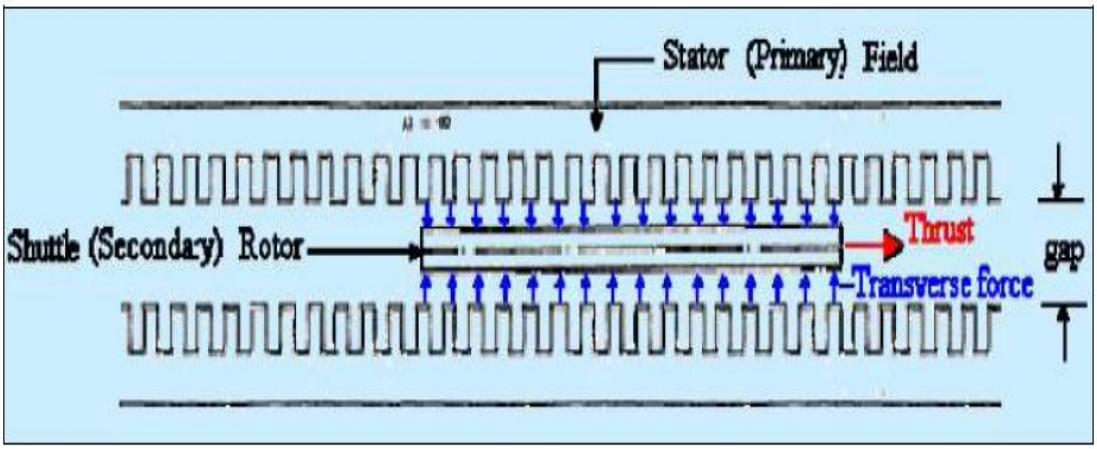

Figure 2.5: Vertical (transverse) forces and thrust on a DSLIM

2.3. Electrical Dynamics Analysis

Dynamic analysis is going to take place for the equivalent circuit model of the LIM, establishing the state-space equation for a better implementation in

further control analysis. Before applying the Kirchhoff's voltages and currents laws for the circuit it will be summarized some important relations for convenience:

From Equation (2.2) we recall the parameter Q which represents the length of the motor on the normalized scale:

$$Q = \frac{DR_{21}(\mathrm{L\,m} + L_{21})}{(\mathrm{L}_1 + L_{21})v_r} \tag{2.8}$$

It will also be defined the function f(Q) as follows:

$$\mathrm{f(Q)}=\frac{\{1-e^{-Q}\}}{Q} \tag{2.9}$$

Now, applying Kirchhoff's laws on the equivalent circuit lead to:

$$I_1 = I_{21} - I_m \tag{2.10}$$

$$\mathrm{V}_1 = I_1 + L_1 \frac{dI_1}{dt} + (I_1 + I_{21}) + \frac{d}{dt}[L_m(1 - f(Q)(I_1 - I_{21})] \tag{2.11}$$

$$0=L_2 \frac{dI_{21}}{dt}+I_{21} \frac{R_{21}}{s}+(I_{21} - I_1)R_{21}f(Q) + \frac{d}{dt}[L_m(1 - f(Q)(I_1 - I_{21})] \tag{2.12}$$

Solving the system equations conduces to the next expressions:

$$[L_m + L_1 \frac{dI_1}{dt}] - L_m[1 - f(Q)]\frac{dI_{21}}{dt}=\mathrm{V}_1\text{-}I_1[\mathrm{R}_1 + R_{21}f(Q) -$$
$$L_m \frac{df(Q)}{dt}]+I_{21}[R_{21}f(Q) - L_m \frac{df(Q)}{dt}]$$
$$-L_m[1 - f(Q)]\frac{dI_1}{dt} + [L_{21} + L_m[1 - f(Q)] \frac{dI_{21}}{dt}] = I_1R_{21}f(Q)\text{-}$$
$$I_{21}[R_{21}f(Q)+\frac{R_{21}}{s}] \tag{2.13}$$

Where s accounts for slip and is defined as:

$$S=\frac{v_s-v_r}{v_s} \tag{2.14}$$

Where v_s is the synchronous speed and it can be formed as:

$$v_s = \frac{2\omega R}{P} = 2f\tau \tag{2.15}$$

Where R is the radius of the rotary induction machine.
τ is the distance between two adjacent poles in the LIM and v_r is the velocity of the rotor. Considering the derivatives of Q and f(Q):

$$\frac{d(Q)}{dt} = \frac{Q}{v_r} * \frac{dv_r}{dt} \tag{2.16}$$

$$\frac{df(Q)}{dt} = \frac{1}{v_r} * \frac{dv_r}{dt}(f(Q) - e^{-Q}) \tag{2.17}$$

Above equations can be simplified using algebraic expressions to allow us have the electrical system differential equations as follows:

$$\frac{dI_1}{dt} = \frac{V_1 - I_1\left[\mathrm{R}_1 + R_{21}f(Q) - L_m\frac{df(Q)}{dt}\right] + I_{21}\left(R_{21}f(Q) - L_m\frac{df(Q)}{dt}\right) + \frac{dI_{21}}{dt}L_m[1-f(Q)]}{L_1 + L_m[1-f(Q)} \tag{218}$$

$$\frac{dI_2}{dt} = \frac{I_1\left[R_{21}f(Q) - L_m\frac{df(Q)}{dt}\right] - I_{21}\left(R_{21}f(Q) + \frac{R_{21}}{s} - L_m\frac{df(Q)}{dt}\right) + \frac{dI_1}{dt}L_m[1-f(Q)]}{L_{21} + L_m[1-f(Q)} \tag{2.19}$$

2.4 mechanical Dynamics analysis

The system will account for the mechanical part assumed as the conventional mass- spring-damper system represent by:

$m\ddot{x} + b\dot{x} + kx = W_{em} — W_d(t)$ (2.20)

In which m is the combined rotor and payload mass, b is the damping linear coefficient and k is some elastic coefficient. W_{em} is the electromagnetic thrust of the LIM and W_d is a disturbance force in time. W_{em} can be found as:

$$W_{em}=3I_{21}^2 R_{21}\frac{\pi}{\omega_2 \tau}-3I_{21}^2 R_{21}\frac{1-e^{-q}}{v\,Q} \quad (2.21)$$

ω_2 is Slip frequency. Then slip can be redefined as:

$$S=\frac{v_s-v_r}{v_s}=\frac{\omega_2}{\omega_1} \quad (2.22)$$

Also from the equivalent circuit we can find the current equation shown below.

$$I_m = I_1 - I_{21} \quad (2.23)$$

CHAPTER THREE

Linear Induction Motor Dynamic Response

3.1 System layout

The layout of the system used to analysis the dynamic response of the LIM is shown in fig 3.1 .The system include the following subsystems.

1. Linear induction motor
2. Mechanical load
3. Electrical source
4. Control system

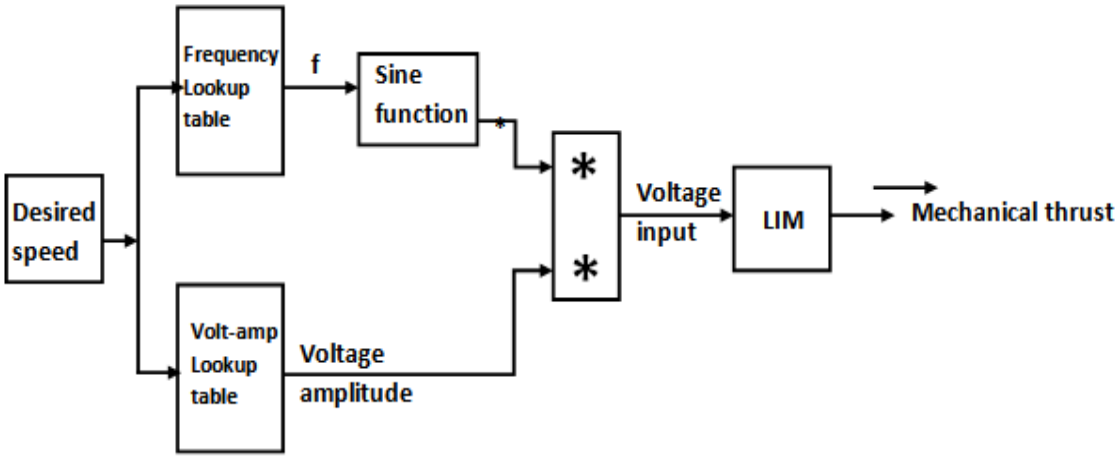

Figure 3.1: System layout

The parameters used for this simulation are shown in Table 3.1.

Table 3.1: Parameters used on the simulation

R_1	R_2	L_2	L_1	L_m	D	T	Q	f(Q)	v_s	v_r	s	V	freq
(ohms)	(ohms)	(H)	(H)	(H)	(m)				(m/s)	(m/s)		(Volt)	(Hz)
0.641	0.332	0.0012	0.0029	-0.064	0.574	.0867	-0.3	1.167	10.4	9.36	0.1	220	60

3.2 Dynamic Response of LIM at No load.

To analysis the response of LIM at steady and transient conditions the model in Figure 3.2 is built in MATLAB/Simulink based on the mathematical model described in chapter two. The parameters in Table 3.1are used as initial values during starting period.

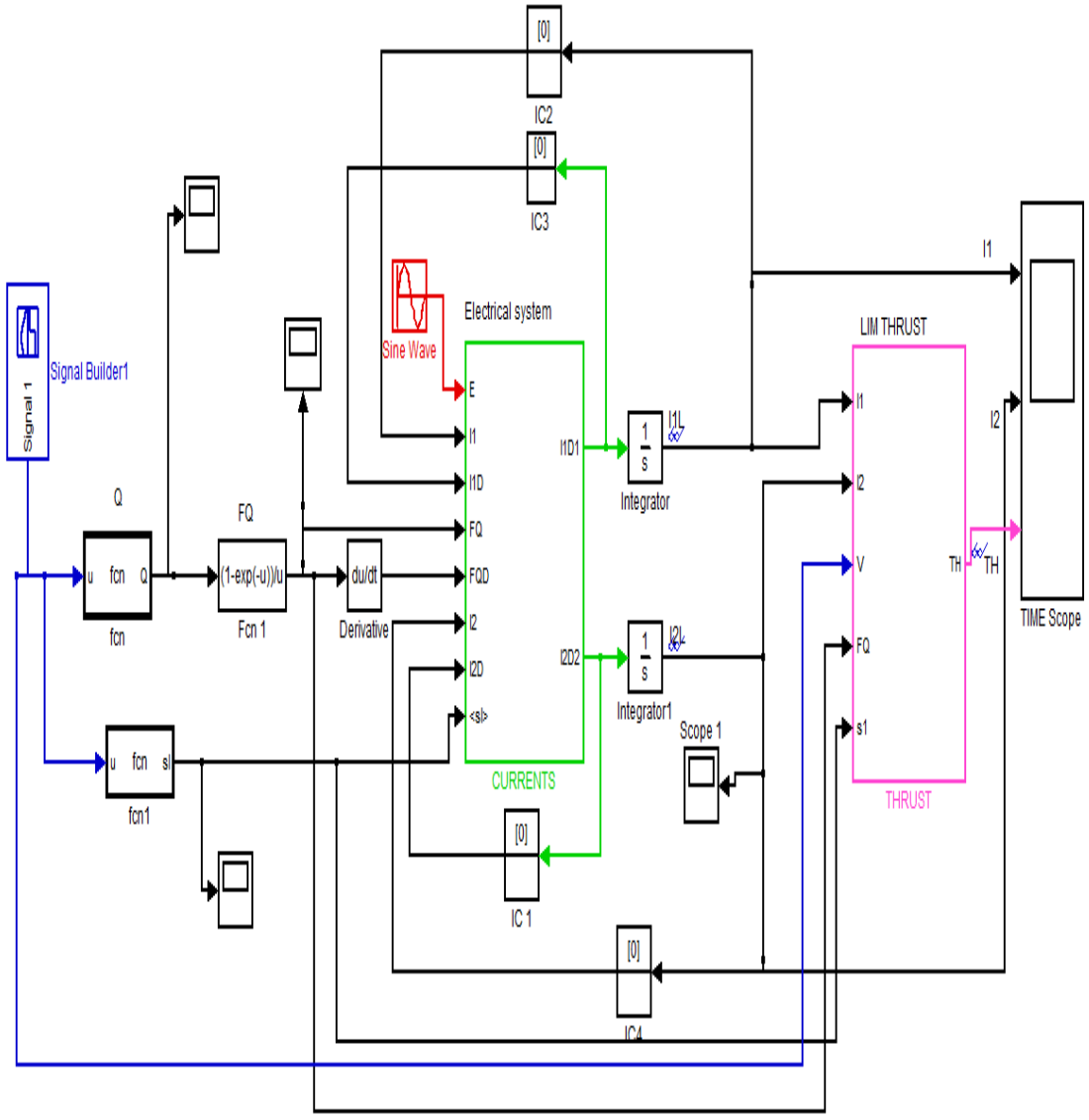

Figure3.2: MATLAB/Simulink model for linear rotor velocity case

Figure 3.3 illustrates the response of the LIM for a varying linear speed of the rotor, starting at 0s and then rising linearly until it reaches a rotor speed of 9.36m/s at a time of 1s remaining constant for 0.5s as shown in Figure 3.3a.

Figure 3.3b corresponds o the response of the stator current (I_1), with a maximum starting current value of 140A and a steady state value of 60A. Figure 3.3c shows the response of the rotor current (I_2), with the same maximum starting current of 140A and a steady state value of 44 A.

On the other hand, the response of the thrust in Figure 3.4d increases progressively from time 0s with a peak value of 1450N until it reaches its maximum of 2550N at 0.8s just before it reach it is steady state at 1s with peak value of 1800N.

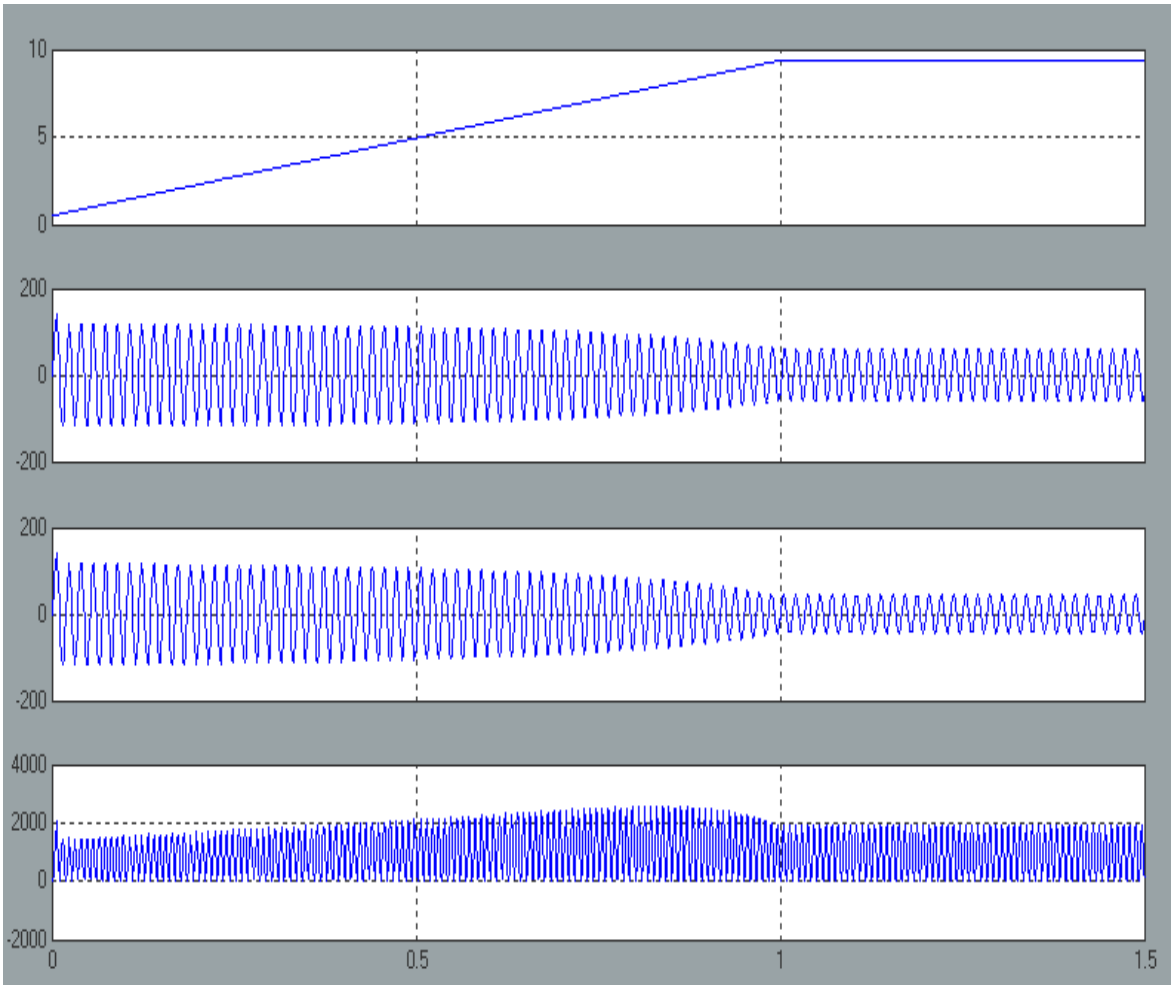

Figure 3.3: From top to bottom: rotor speed, primary current, secondary current, and thrust.

3.3 Thrust Control of LIM Using Lookup Tables.

The following analysis is going to be developed assuming a steady state of the system where the frequency (f), the rotor speed (v_r) and the thrust (Th) are going to be invariable through time. The mechanical system is not yet included at this instance. Figure 3.4 shows the MATLAB/Simulink model for thrust control of LIM using Lookup Tables.

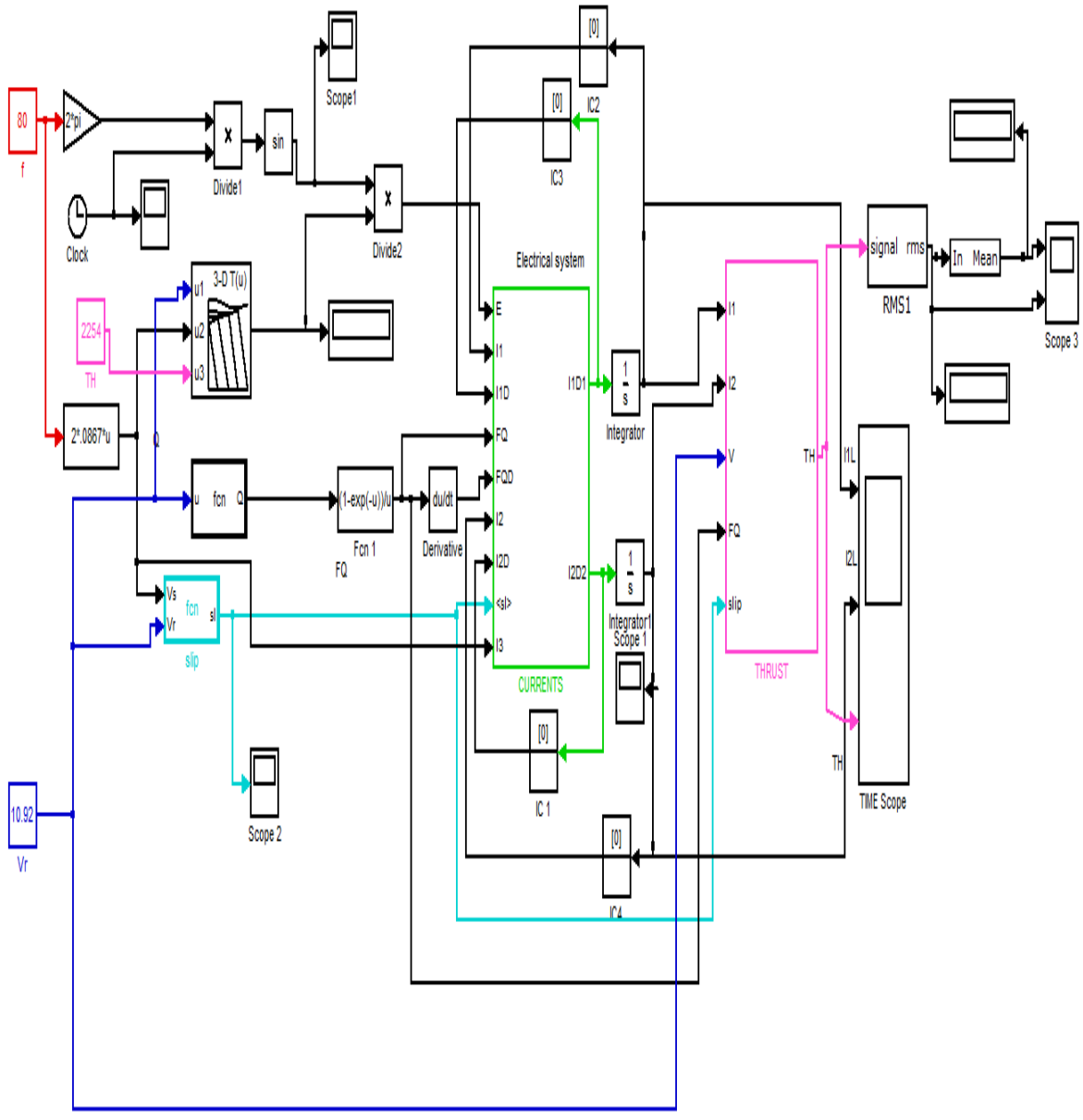

Figure 3.4:MATLAB/Simulink model for thrust control of LIM using Lookup Tables

To get a specific thrust from the LIM the Lookup table will choose the correct value of voltage amplitude (Vol) using combination of the synchronous speed and a set value of thrust , by using trilinear interpolation with a specific MATLAB/Simulink block called Lookup table n-D (3-D in this case). Then this value is going to multiply the sinusoidal signal from which the frequency can be changed from an outer block in the model. The overall signal is going to be the input of the electrical system from which a close value of actual thrust compared to the reference thrust is expected. The objective of this model is to obtain an actual thrust as set by the reference value using Lookup table. The thrust response of the system is determined by varying parameters such as frequency (f), Rotor speed (v_r) and voltage amplitude (Vol). The stepwise procedures is developed as follows:

1) Define the intervals of v_s, v_r and Vol for which the thrust needs to be defined as shown in Table 3.2:

Table 3.2 Values of v_s, v_r and Vol for which the thrust needs to be defined

v_s	10.4	12.14	13.87	15.61	17.34
v_r	9.36	10.92	12.48	14.05	15.61
Vol	100	200	300	400	500

2) Get the values of thrust for each combination of v_s, v_r and V_{ol} as shown in Table 3.3.

Table 3.3 thrust for each combination of v_s, v_r and V_{ol}

Vs	Vr	Vol	TH	Slip	freq
10.4	9.36	100	223	0.1	60
10.4	9.36	200	892	0.1	60
10.4	9.36	300	2008	0.1	60
10.4	9.36	400	3570	0.1	60
10.4	9.36	500	5576	0.1	60
10.4	10.92	x	x	X	60
10.4	12.48	x	x	X	60
10.4	14.05	x	x	X	60
10.4	15.61	x	x	X	60
12.14	9.36	100	223.5	0.23	70
12.14	9.36	200	894	0.23	70
12.14	9.36	300	2012	0.23	70
12.14	9.36	400	3577	0.23	70
12.14	9.36	500	5590	0.23	70
12.14	10.92	100	173.4	0.1	70
12.14	10.92	200	693.7	0.1	70
12.14	10.92	300	1561	0.1	70
12.14	10.92	400	2775	0.1	70
12.14	10.92	500	4336	0.1	70
12.14	12.48	x	x	X	70
12.14	14.05	x	x	X	70
12.14	15.61	x	x	X	70
13.87	9.36	100	155.3	0.33	80
13.87	9.36	200	622.5	0.33	80
13.87	9.36	300	1404	0.33	80
13.87	9.36	400	2485	0.33	80
13.87	9.36	500	3902	0.33	80
13.87	10.92	100	168.9	0.21	80
13.87	10.92	200	675.7	0.21	80

Vs	Vr	Vol	TH	slip	freq
15.61	9.36	500	2648	0.4	90
15.61	10.92	100	119.6	0.3	90
15.61	10.92	200	478.3	0.3	90
15.61	10.92	300	1077	0.3	90
15.61	10.92	400	1921	0.3	90
15.61	10.92	500	2990	0.3	90
15.61	12.48	100	130.1	0.2	90
15.61	12.48	200	519.5	0.2	90
15.61	12.48	300	1172	0.2	90
15.61	12.48	400	2084	0.2	90
15.61	12.48	500	3256	0.2	90
15.61	14.05	100	110.2	0.1	90
15.61	14.05	200	440.8	0.1	90
15.61	14.05	300	991.4	0.1	90
15.61	14.05	400	1761	0.1	90
15.61	14.05	500	2755	0.1	90
15.61	15.61	X	0	x	90
17.34	9.36	100	73.5	0.46	100
17.34	9.36	200	294	0.46	100
17.34	9.36	300	661.5	0.46	100
17.34	9.36	400	1176	0.46	100
17.34	9.36	500	1838	0.46	100
17.34	10.92	100	82.84	0.37	100
17.34	10.92	200	331.3	0.37	100
17.34	10.92	300	745.5	0.37	100
17.34	10.92	400	1325	0.37	100
17.34	10.92	500	2071	0.37	100
17.34	12.48	100	93.6	0.28	100
17.34	12.48	200	374.5	0.28	100

13.87	10.92	300	1517	0.21	80
13.87	10.92	400	2693	0.21	80
13.87	10.92	500	4210	0.21	80
13.87	12.48	100	137.4	0.1	80
13.87	12.48	200	550	0.1	80
13.87	12.48	300	1235	0.1	80
13.87	12.48	400	2202	0.1	80
13.87	12.48	500	3435	0.1	80
13.87	14.05	x		X	80
13.87	15.61	x		X	80
15.61	9.36	100	105.5	0.4	90
15.61	9.36	200	422.7	0.4	90
15.61	9.36	300	950.9	0.4	90
15.61	9.36	400	1691	0.4	90
17.34	12.48	300	842.5	0.28	100
17.34	12.48	400	1498	0.28	100
17.34	12.48	500	2341	0.28	100
17.34	14.05	100	102.1	0.19	100
17.34	14.05	200	408.3	0.19	100
17.34	14.05	300	918.7	0.19	100
17.34	14.05	400	1633	0.19	100
17.34	14.05	500	2552	0.19	100
17.34	15.61	100	89.65	0.1	100
17.34	15.61	200	358.8	0.1	100
17.34	15.61	300	806.8	0.1	100
17.34	15.61	400	1434	0.1	100
17.34	15.61	500	2241	0.1	100

The previous table gives some values that defined the response of the trust for different combinations of v_s. v_r and Vol.

3) After this table has been complete, a trilinear interpolation is used in order to define the thrust response for different values of the voltage amplitude in a range from 100 to 500 as defined in step 1. Table 3.4 shows Thrust matrix with dimensions 5x5x5.

Table 3.4 : Thrust matrix with dimensions 5x5x5

v=100	10.4	12.14	13.87	15.61	17.34	x =Vs
9.36	223.1	223.5	155.3	105.5	73.5	
10.92	0	173.4	168.9	119.6	82.84	
12.48	0	0	137.4	130.1	93.6	
14.05	0	0	0	110.2	102.1	
15.61	0	0	0	0	89.65	

y =Vr

v=200	10.4	12.14	13.87	15.61	17.34
9.36	892.5	894	622.5	422.7	294
10.92	0	693.7	675.7	478.3	331.3
12.48	0	0	550	519.5	374.5
14.05	0	0	0	440.8	408.3
15.61	0	0	0	0	358.8

v=300	10.4	12.14	13.87	15.61	17.34
9.36	2008	2012	1404	950.9	661.5
10.92	0	1561	1517	1077	745.5
12.48	0	0	1235	1172	842.5
14.05	0	0	0	991.4	918.7
15.61	0	0	0	0	806.8

v=400	10.4	12.14	13.87	15.61	17.34
9.36	3570	3577	2485	1691	1176
10.92	0	2775	2693	1921	1325
12.48	0	0	2202	2084	1498
14.05	0	0	0	1761	1633
15.61	0	0	0	0	1434

v=500	10.4	12.14	13.87	15.61	17.34
9.36	5576	5590	3902	2648	1838
10.92	0	4336	4210	2990	2071
12.48	0	0	3435	3256	2341
14.05	0	0	0	2755	2552
15.61	0	0	0	0	2241

Vs2 and Vr2 are defined by each possible combination between each other and Vo12=values of voltage amplitudes from 100 to 500 with a step of 10. This procedure generates a list of TH2 for each possible combination between Vs2 and Vr2.

4) Define a range of thrust for the system. The range was defined by the last set of values of thrust from Table 3.3. Thus a new table needs to be created where the inputs are v_s, v_r and thrust and the output is the voltage amplitude Vol. To build this table. One last interpolation is needed. This time is a l-D interpolation between the values of Th2 and Vol2 for each set of thrust values chose, once this is complete a table like Table 3.4 is built.

5) The last trilinear interpolation is made by using the 3-D Lookup table MATLAB/Simulink block in which the data must be defined the same way as when using the interp3 MATLAB function explained in step 3, information are shown in the sequel:

Vs1=[l0.40 12.14 13.87 15.61 17.34]

Vr1=[9.36 10.92 12.48 14.05 15.61]

Thl=[89.9 360.7 811.5 1439 2254]

Vol1 is defined by a 3D matrix of 5x5x5 based on the information on Table 3.5 and is shown in Table 3.6.

Table 3.5: Voltage amplitude for each combination of $v_s, v_r$and Thrust

freq	Vs	Vr	TH	Vol
60	10.4	9.36	89.65	80.065
60	10.4	9.36	358.8	120.27
60	10.4	9.36	806.8	187.13
60	10.4	9.36	1434	248.54
60	10.4	9.36	2241	314.82
60	10.4	10.92	x	0
60	10.4	12.48	x	0
60	10.4	14.05	x	0
60	10.4	15.61	x	0
70	12.14	9.36	89.65	80.038
70	12.14	9.36	358.8	120.18
70	12.14	9.36	806.8	186.93
70	12.14	9.36	1434	248.3
70	12.14	9.36	2241	314.53

freq	Vs	Vr	TH	Vol
90	15.61	9.36	2241	457.47
90	15.61	10.92	89.65	91.651
90	15.61	10.92	358.8	166.68
90	15.61	10.92	806.8	254.87
90	15.61	10.92	1434	342.3
90	15.61	10.92	2241	429.93
90	15.61	12.48	89.65	89.612
90	15.61	12.48	358.8	158.73
90	15.61	12.48	806.8	244.03
90	15.61	12.48	1434	328.73
90	15.61	12.48	2241	413.32
90	15.61	14.05	89.65	93.784
90	15.61	14.05	358.8	175.21
90	15.61	14.05	806.8	266.47

70	12.14	10.92	89.65	83.904
70	12.14	10.92	358.8	135.63
70	12.14	10.92	806.8	212.86
70	12.14	10.92	1434	285.3
70	12.14	10.92	2241	356.01
70	12.14	12.48	x	0
70	12.14	14.05	x	0
70	12.14	15.61	x	0
80	13.87	9.36	89.65	85.948
80	13.87	9.36	358.8	143.56
80	13.87	9.36	806.8	223.63
80	13.87	9.36	1434	303.13
80	13.87	9.36	2241	377.44
80	13.87	10.92	89.65	84.363
80	13.87	10.92	358.8	137.47
80	13.87	10.92	806.8	215.42
80	13.87	10.92	1434	290.14
80	13.87	10.92	2241	361.56
80	13.87	12.48	89.65	88.427
80	13.87	12.48	358.8	153.66
80	13.87	12.48	806.8	237.48
80	13.87	12.48	1434	320.59
80	13.87	12.48	2241	403.42
80	13.87	14.05	x	0
80	13.87	15.61	x	0
90	15.61	9.36	89.65	95.003
90	15.61	9.36	358.8	179.86
90	15.61	9.36	806.8	272.73
90	15.61	9.36	1434	365.27
90	15.61	14.05	1434	357.51
90	15.61	14.05	2241	448.29
90	15.61	15.61	X	0
100	17.34	9.36	89.65	107.32
100	17.34	9.36	358.8	217.54
100	17.34	9.36	806.8	328.25
100	17.34	9.36	1434	438.97
100	17.34	9.36	2241	560.88
100	17.34	10.92	89.65	107.32
100	17.34	10.92	358.8	217.54
100	17.34	10.92	806.8	328.25
100	17.34	10.92	1434	438.97
100	17.34	10.92	2241	560.88
100	17.34	12.48	89.65	98.594
100	17.34	12.48	358.8	194.63
100	17.34	12.48	806.8	292.47
100	17.34	12.48	1434	390.24
100	17.34	12.48	2241	488.14
100	17.34	14.05	89.65	95.934
100	17.34	14.05	358.8	183.78
100	17.34	14.05	806.8	278.09
100	17.34	14.05	1434	372.15
100	17.34	14.05	2241	466.16
100	17.34	15.61	89.65	100
100	17.34	15.61	358.8	200
100	17.34	15.61	806.8	300
100	17.34	15.61	1434	400
100	17.34	15.61	2241	500

A trilinear interpolation is used in order to define the thrust response for different values of the voltage amplitude as shown in Table 3.5.

Table 3.6: Vol matrix with dimensions 5x5x5

th=89.65	10.4	12.14	13.87	15.61	17.34	x=Vs
9.36	80.06	80.04	85.95	95	107.3	
10.92	0	83.9	84.36	91.65	107.3	
12.48	0	0	88.43	89.61	98.59	
14.05	0	0	0	93.78	95.93	
15.61	0	0	0	0	100	
y=Vr						

th=358.8	10.4	12.14	13.87	15.61	17.34
9.36	120.3	120.2	143.6	179.9	217.5
10.92	0	135.6	137.5	166.7	217.5
12.48	0	0	153.7	158.7	194.6
14.05	0	0	0	175.2	183.8
15.61	0	0	0	0	200

th=806.8	10.4	12.14	13.87	15.61	17.34
9.36	187.1	186.9	223.6	272.7	328.3
10.92	0	212.9	215.4	254.9	328.3
12.48	0	0	237.5	244	292.5
14.05	0	0	0	266.5	278.1
15.61	0	0	0	0	300

th=1434	10.4	12.14	13.87	15.61	17.34
9.36	248.5	248.3	303.1	365.3	439
10.92	0	285.3	290.1	342.3	439
12.48	0	0	320.6	328.7	390.2
14.05	0	0	0	357.5	372.1
15.61	0	0	0	0	400

th=2241	10.4	12.14	13.87	15.61	17.34
9.36	314.8	314.5	377.4	457.5	560.9
10.92	0	356	361.6	429.9	560.9
12.48	0	0	403.4	413.3	488.1
14.05	0	0	0	448.3	466.2
15.61	0	0	0	0	500

After the previous information is defined, one can proceed to enter it on the Lookup table MATLAB/Simulink block, from which the inputs are v_s, v_r and a reference value of thrust (Th). and the output will be a voltage amplitude (Vol). as shown in Figure 3.7.

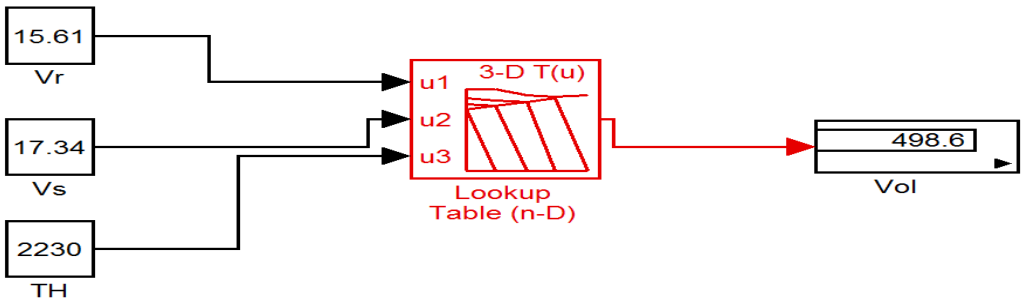

Figure 3.5: 3-D Lookup table MATLAB/Simulink block

7) A verification of the procedure is going to be developed in the sequel for a set of arbitrary inputs. The results are summarized in Table 3.7.

Table 3.7: System verification by using 3-d Lookup tables

f	v_s	v_r	ref_TH	Vol	actual_TH	Error	Fig
60	10.4	9.36	360.7	120.6	324.6	10.00832	
70	12.14	10.92	550	168.6	492.9	10.38182	
80	13.87	12.48	1200	289.6	1152	4	
90	15.61	14.05	1800	398.7	1750	2.777778	
100	17.34	15.61	2230	498.6	2229	0.044843	

Table 3.7 shows the inputs v_s, v_r and Ref_Th (reference value of thrust) and compares this last one with the actual thrust response of the system. One can see how the error tends to diminish while increasing the speed values which can be expected provided that the range of thrust was chose based on the thrust values for a synchronous speed of 17.34m/s as explained in step 4. This however, would be a first approach on controlling the thrust in a LIM for these particular conditi7ns.

3.4 Simulation of a LIM as Electromechanical System

At this point, the value of the rotor speed v_r is no longer going to be assumed. Instead, the mechanical response is going to account for the overall response of the system as shown in Figure 3.6 and will be assumed as the conventional

mass-spring-damper system represent by Equation (2.20). Table 3.2 shows the electrical and physical characteristics of the motor.

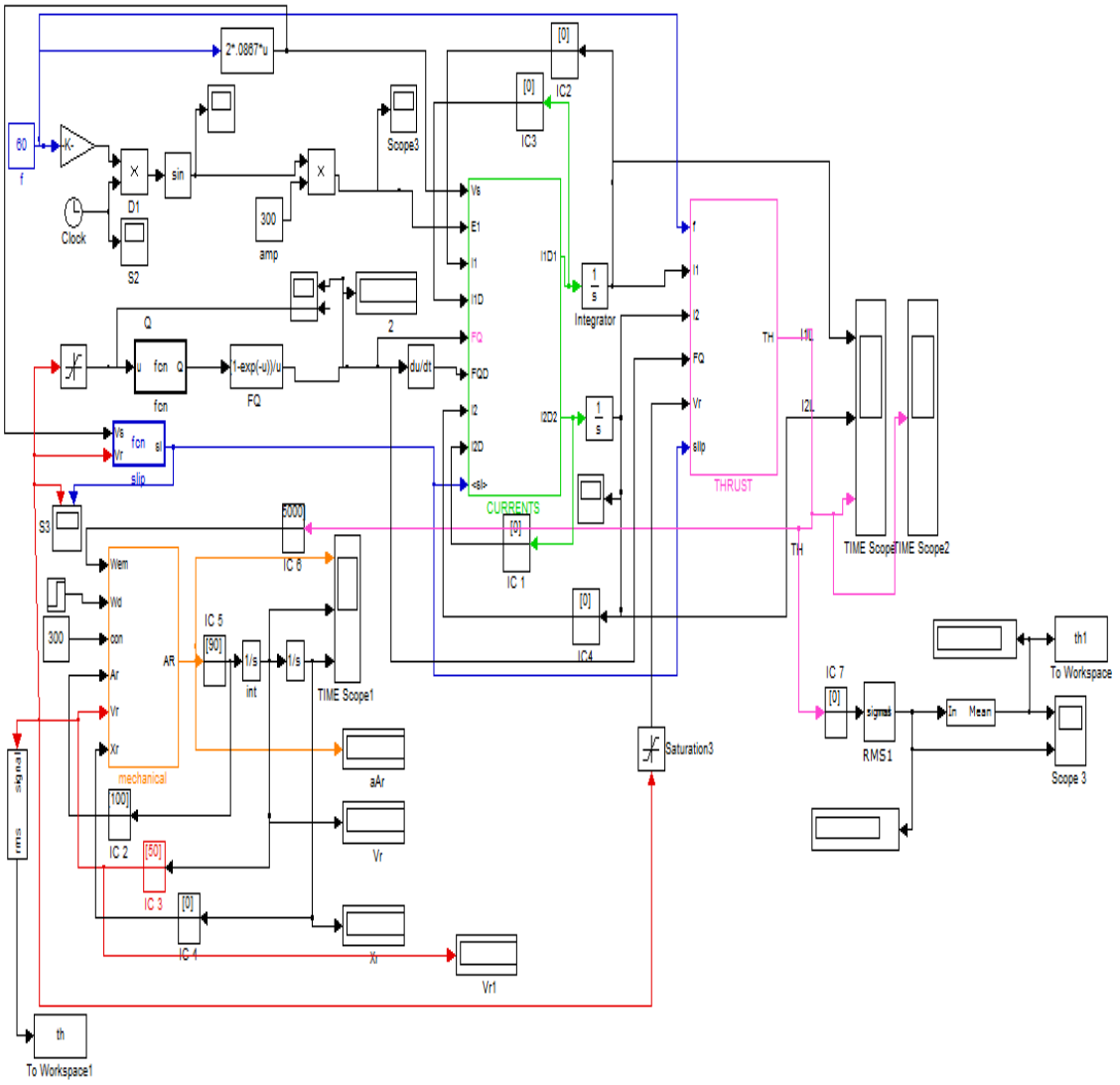

Figure 3.6: MATLAB/Simulink model for the electromechanical system

Table 3.8 below show the parameters used on electromechanical system simulation

Table 3.8: Parameters used on electromechanical system simulation

R_1	R_2	L_1	L_2	L_m	D	τ	v_s	m	V	Freq
(ohms)	(ohms)	(H)	(H)	(H)	(m)		(m/s)	kg	(Volts)	(Hz)
0.641	0.332	0.0012	0.0029	-0.064	0.574	0.0867	10.4	300	300	60

The responses in time of stator and rotor currents are shown in Figure 3.7 alongside rotor speed. The initial maximum peak value is more than 200A for both currents at the start when the rotor speed is zero. After the rotor starts the current decays to less than half the value of the maximum and maintain this value until they start to decay once again in a progressive way until they reach the steady state value.

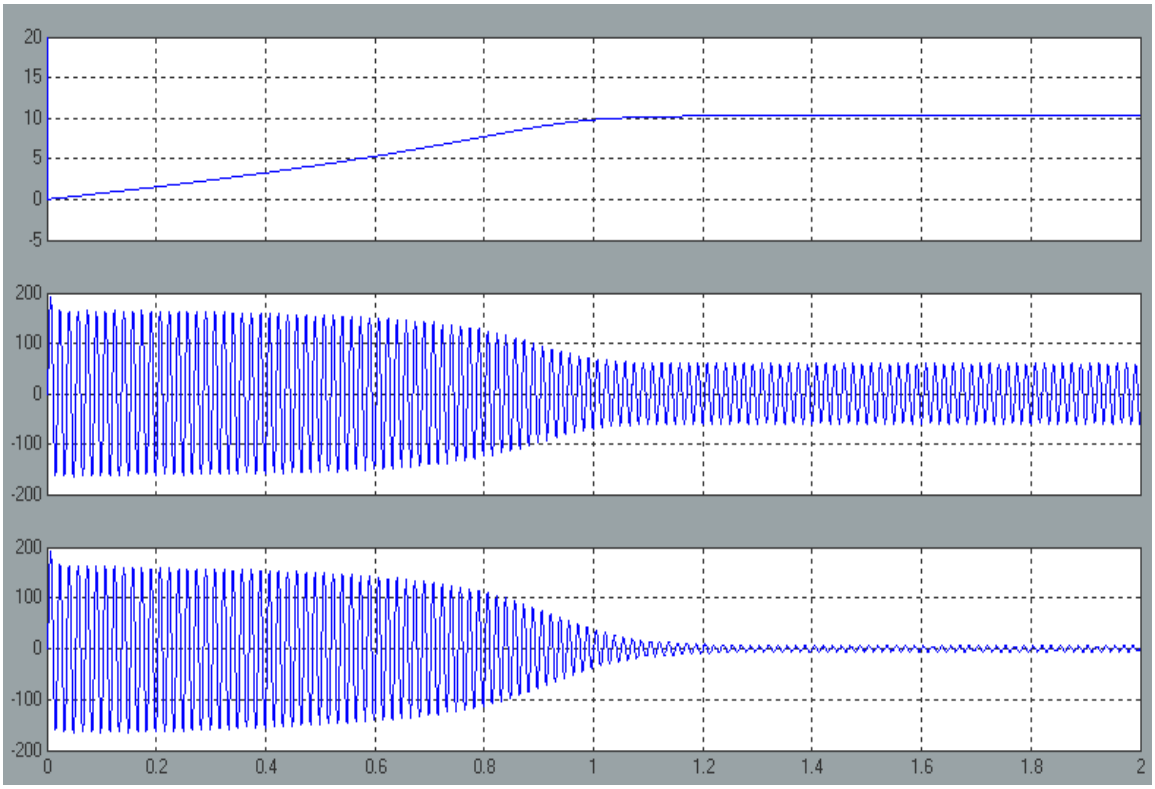

Figure 3.7: Stator and rotor currents response in time of the LIM

Figure 3.8 shows the response of the thrust over time in which a maximum peak value of 8000N stand out at the starting stage. Soon afterwards the thrust response decays rapidly until it reaches its lowest value and from this point on it begins to increase gradually until it reaches a maximum value at time 1s. time at which it begins to decay once again until it reaches the steady state value around 0N.

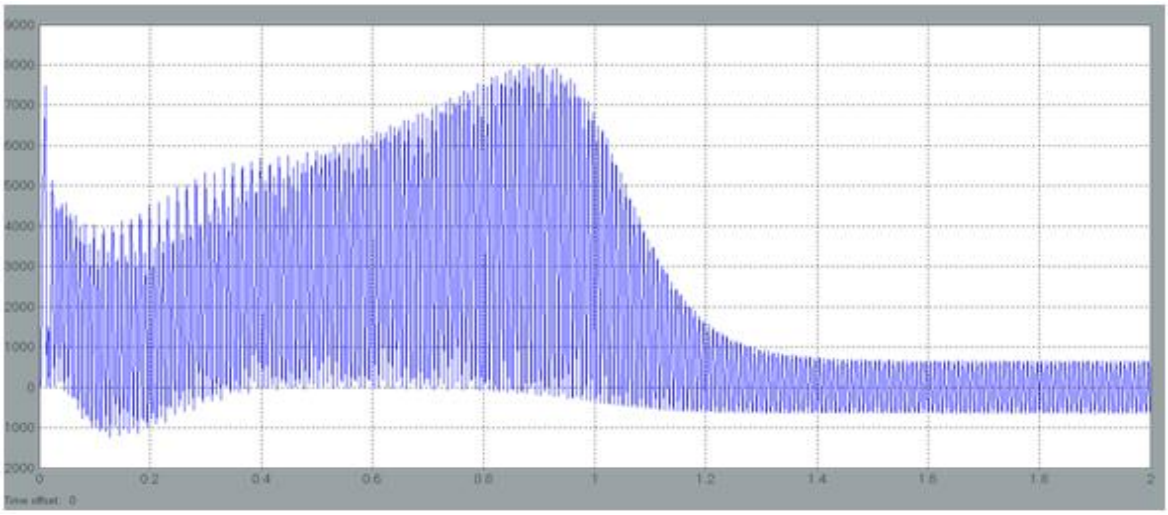

Figure 3.8. Thrust response in time of the LIM

Figure 3.9 shows the response of the acceleration, speed and position of the rotor. The acceleration behaves the same way as the thrust does with a maximum peak value of 30m/s at the initial stage. The speed stalls at zero and makes an abrupt jump corresponding to the acceleration peak and then it traces a smooth path which increases gradually until it stabilizes at the steady state value around 10.36m/s. The position is traced by a smooth and progressive path which starts at 0m and reaches 7m when the motor reaches the steady state. And after 2s the rotor has traveled around 13m.

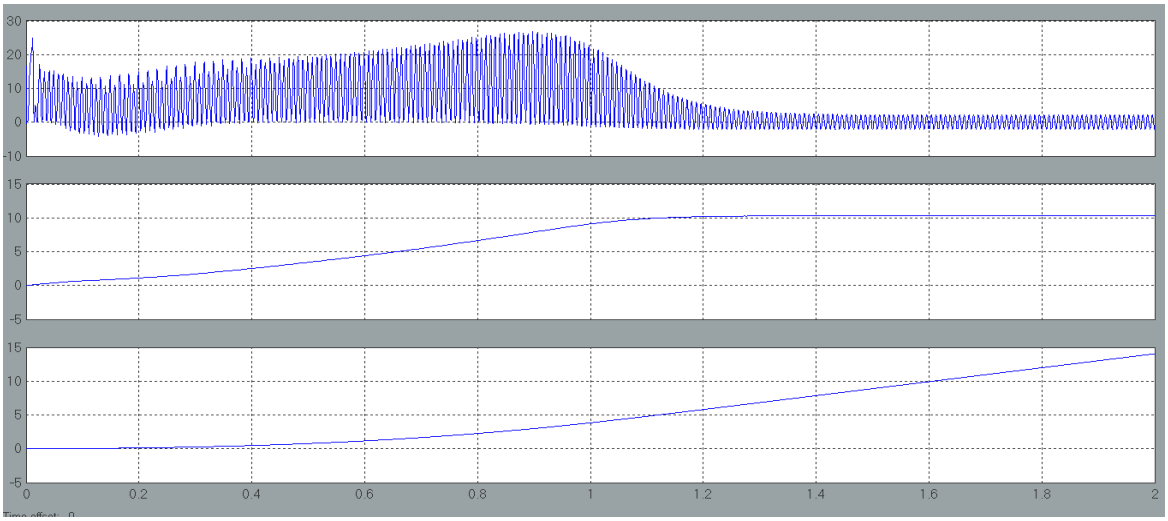

Figure 3.9: Acceleration, speed and position response in time of the rotor

Figure 3.10 shows the response of the thrust by varying the speed of the rotor. It can be notice once again a maximum peak value at the initial stage with a value 5570N which drops rapidly to 250N and then starts to increase faster until it reaches some value around 3000N. time at which it continue increasing slower until it reaches a maximum value around 4470N and then begin to decay quickly until it reaches 0N. time at which the rotor speed has reached the synchronous speed and remains in steady state. So thrust is no longer needed. Two main zones can be identified from the Figure. The transient and the steady state zone. The transient is due to the intrinsic nonlinearities of the system as well as the startup characteristics of the LIM. One also can notice that the LIM is being operating in the motoring region. So no electric power generation is present.

Figure 3.12 shows the Mean thrust versus rotor speed response of the LIM.

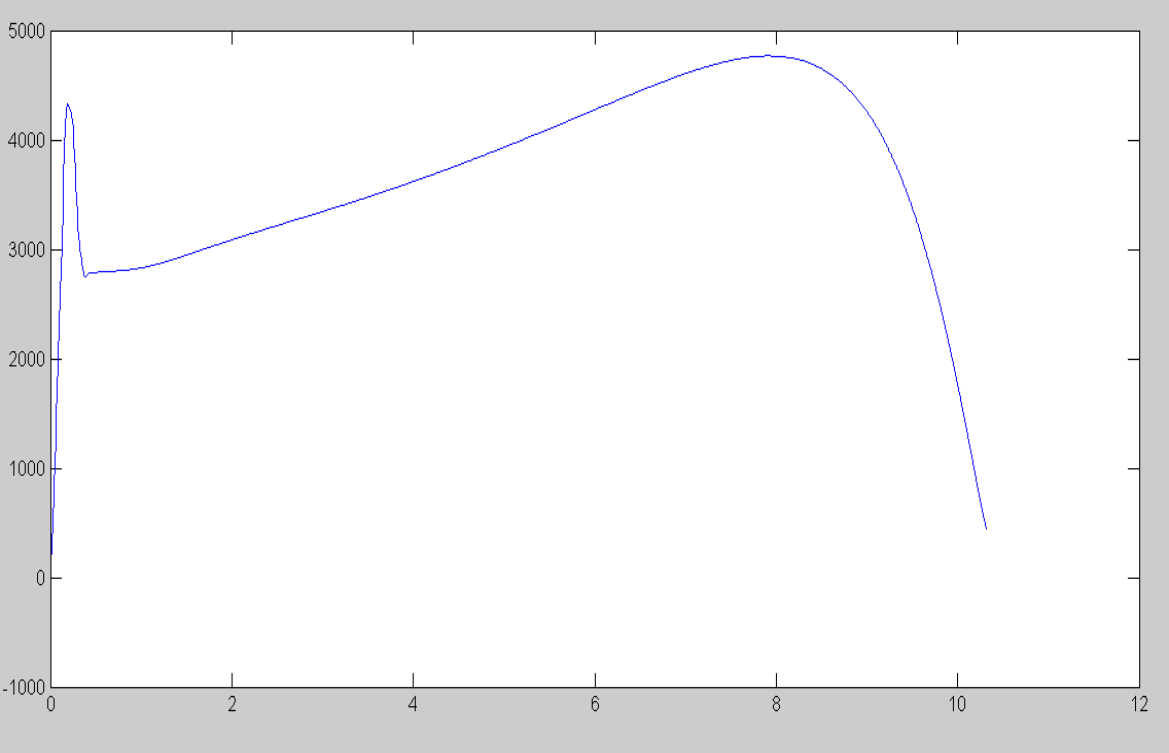

Figure 3.10: Mean thrust versus rotor speed response of the LIM

3.5 Speed Control of LIM Using Lookup table

The objective of the following simulation is to set a reference value of rotor speed as an input to the system. The parameters of the motor are going to be the same as the ones in Table 3.1 except for the frequency and voltage amplitude values which are going to vary to allow the system to reach the desired conditions. A disturbing force is also added to the mechanical system all the time with a constant value of W_d = 1000N.

Figure 3.11 illustrates the MATLAB/Simulink model for the LIM accounting for the new block set.

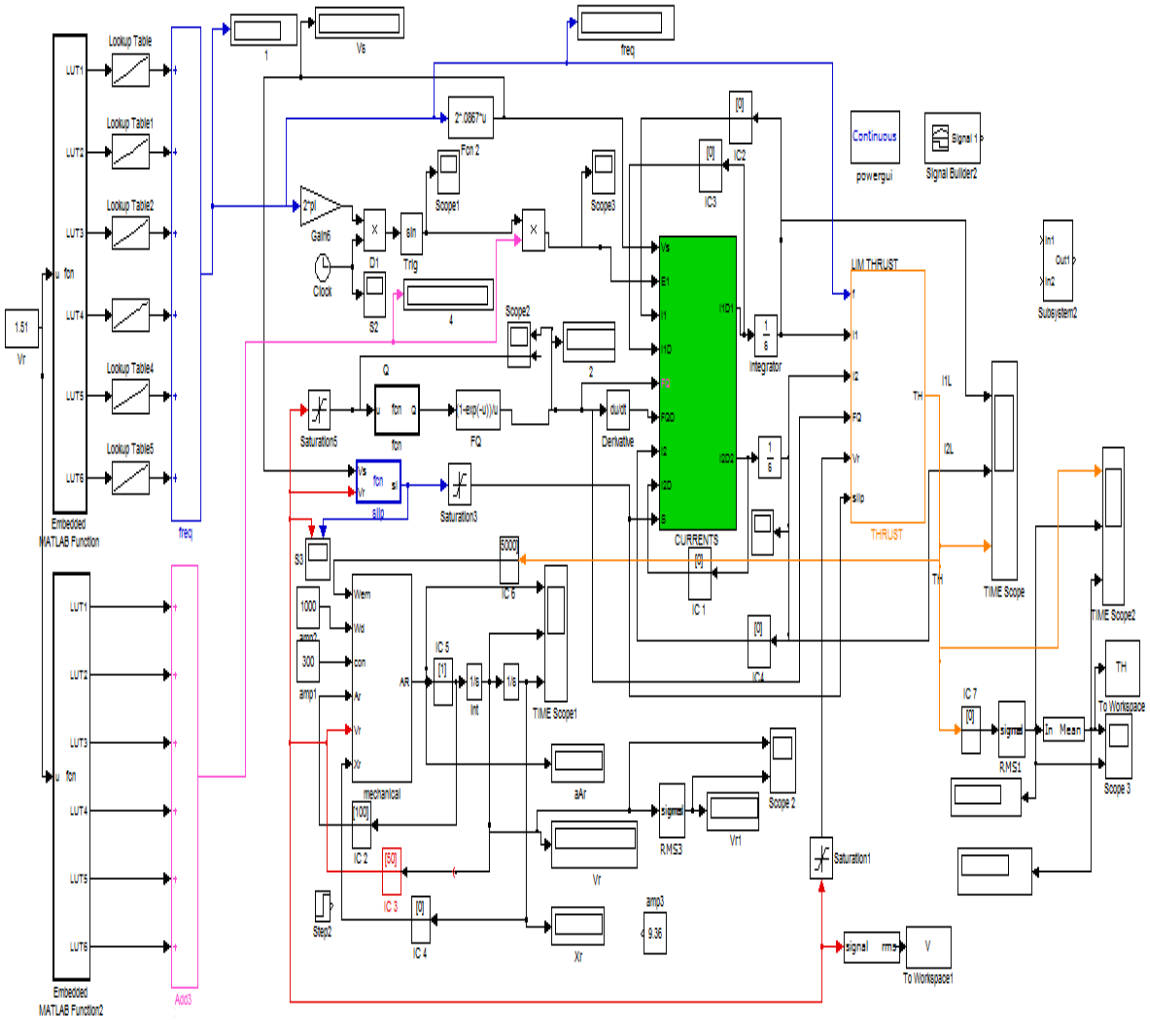

Figure 3.11: MATLAB/Simulink model of the LIM using Lookup tables to set a desired rotor speed

For LIM speed control Lookup table Implementation the following steps were carried out:

l) Values of frequency were taken for different voltage amplitudes (50, 100, 200, 300, 400, 500 Volts) under the criterion that the steady state had to be reached before 2 seconds. These values are shown in Table 3.7 as follows:

Table 3.7: Rotor speed values for each f, Vol combination.

amplitude=50 volt				
F	Vr	Vs	S	S.S T
0	0	0	0	<2sec
3	0.478	0.5202	0.080738	<2sec
5	0.795	0.867	0.082584	<2sec
8	1.227	1.3872	0.115484	<2sec
10	1.445	1.734	0.166667	>2sec
amplitude=100 volt				
F	Vr	Vs	S	S.S T
10	1.668	1.734	0.038062	<2ec
13.5	2.232	2.3409	0.046521	<2ec
17	2.772	2.9478	0.059638	<2ec
20	3.215	3.468	0.072953	<2ec
23	3.634	3.9882	0.088812	<2ec
26	3.998	4.5084	0.113211	>2sec
amplitude=200 volt				
F	Vr	Vs	S	S.S T
26	4.384	4.5084	0.027593	<2sec
29	4.875	5.0286	0.030545	<2sec
33	5.523	5.7222	0.034812	<2sec
36	6.003	6.2424	0.038351	<2sec
39	6.477	6.7626	0.042232	<2sec
42	6.946	7.2828	0.046246	>2sec

amplitude=300 volt				
f	Vr	Vs	s	S.S T
42	7.108	6.6024	0.071131	<2sec
45	7.603	7.803	-0.02631	<2sec
49	8.258	8.4966	-0.02889	<2sec
52	8.747	9.0168	-0.03084	<2sec
55	9.233	9.537	-0.03293	<2sec
58	9.716	10.0572	-0.03512	<2sec
60	10.04	10.404	-0.03625	>2sec
amplitude=400 volt				
f	Vr	Vs	s	S.S T
60	10.16	9.432	0.071654	<2sec
63	10.66	10.9242	-0.02478	<2sec
66	11.15	11.4444	-0.0264	<2sec
69	11.63	11.9646	-0.02877	<2sec
72	12.14	12.4848	-0.0284	>2sec
amplitude=500 volt				
f	Vr	Vs	s	S.S T
72	12.23	11.3184	0.074538	<2sec
74	12.57	12.8316	-0.02081	<2sec
77	13.06	13.3518	-0.02234	<2sec
80	13.56	13.872	-0.02301	<2sec
83	14.05	14.3922	-0.02436	<2sec
85	14.38	14.739	-0.02497	>2sec

Table 3.7 shows all the range of rotor speeds covered from 0m/s to 14.38m/s, for a frequency range from 0Hz to 85Hz and a voltage magnitude from 50V to 500V. Each of these values were obtain under the criterion mentioned before, in which the steady state was reached before 2s.

2) Create a 1-D Lookup table for each of the six previous tables. By making this, a range of frequency from 0 to 85Hz is covered which implies a range from 0m/s to 14.38m/s covered for the desired speed of the rotor. However, values larger than 14.473 m/s can also be set provided that the Lookup tables allow extrapolation in which case the Lookup table corresponding to voltage amplitude of 500V would be used although the steady state would not be reached before 2seconds, that is, it would not obey to the efficiency criterion. This means that if the desired speed is Vr 5.7m/s, the Lookup table corresponding to a voltage amplitude of 200V will be used and the frequency will be somewhere between 33Hz and 36Hz. thus, one can see the need to demultiplex the input v_r for one of the six Lookup tables depending on its value.

3) Demultiplex v_r to select the corresponding Lookup table and get the optimum frequency value. Figure 3.13 shows the blocks corresponding to the demultiplex action in which an arbitrary value of rotor speed (v_r) is set and a specific Lookup table is implemented depending on the range of voltage amplitude and frequency v_r is located. After the optimum Lookup table is chosen, they output the value of frequency to be part of the sinusoidal voltage source that enters in the electrical block. In Figure 3.13 one can see another demultiplex implementation for which an optimum value of amplitude voltage is set upon the range under the reference value of v_r is covered. At this point, the voltage source of the system is completely defined, and the actual rotor speed value of the system is expected to be really close from the reference value, v_r, after the system reaches the steady state, which of course must be before 2s, as established in step 1.

4) Validation of the simulation recalling the parameters of the model we have: desired v_r=12m/s, Wd=1000 N, b=0 and c=0,

Figure 3.12 shows the response in time of the stator and the rotor currents. One can see an initial maximum peak value of almost 200A for both currents at the staff, when the speed rotor is zero After the rotor starts moving the current has a small decay and maintain this value until they start to decay once again in a progressive way until they reach the steady state value. One can notice that in the case of the rotor speed, the steady state value is very close to zero provided that the synchronous speed of the LIM has been reached so there is no longer current demand.

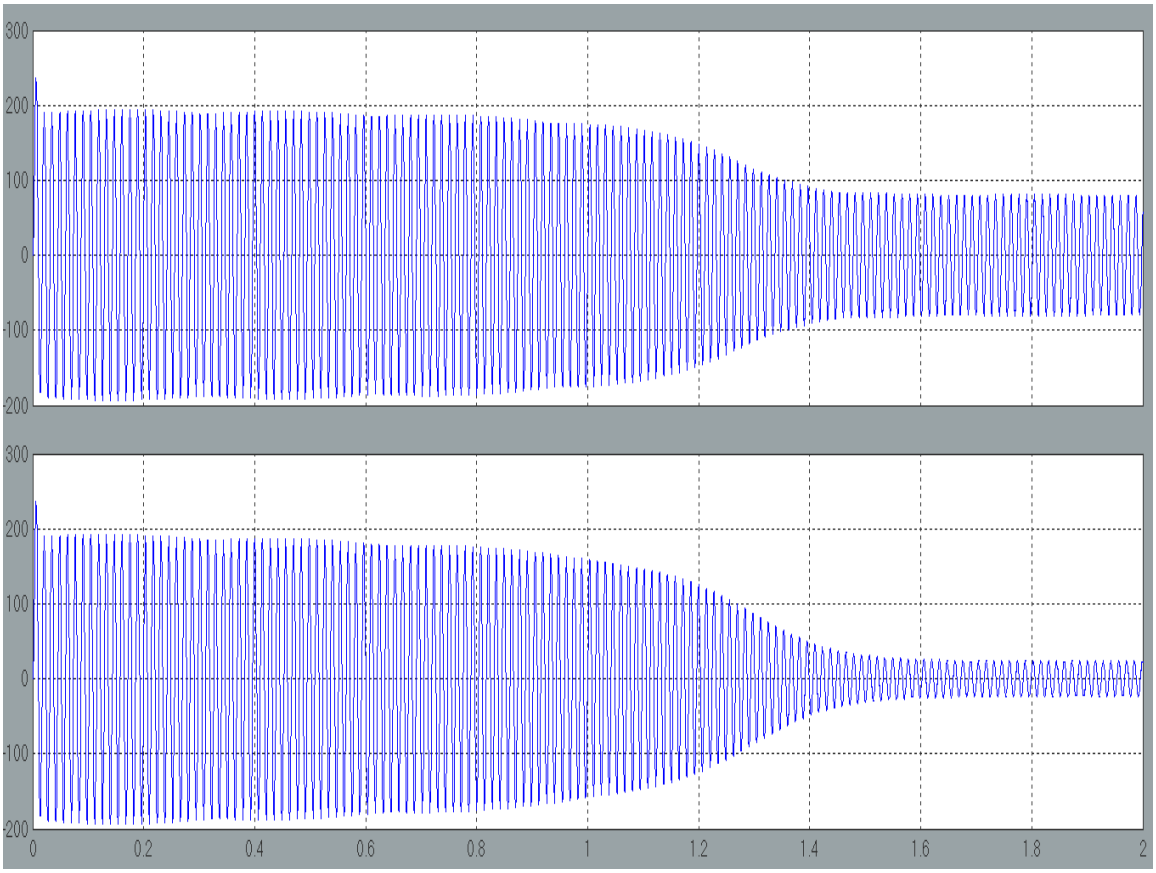

Figure. 3.12: Stator and rotor current responses using Lookup tables

Figure 3.13 shows the response of the thrust over time (instantaneous thrust) in which a maximum peak value of 7800N stands out at the starting stage, the

same way as the stator and rotor currents do. Soon afterwards the thrust response has a small decay rapidly until it reaches its lowest value and from this point on it begins to increase gradually until it reaches a maximum value of 10000N at time 1.2s, time at which it begins to decay until it reaches the steady state response.

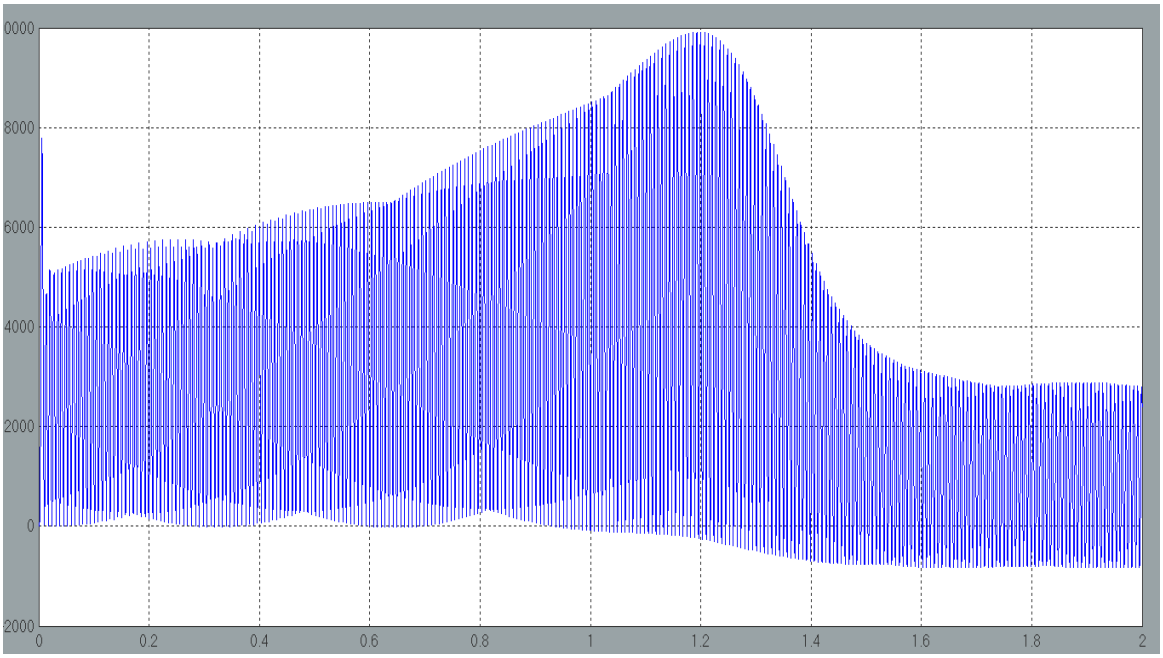

Figure 3.13. Thrust response in time of the LIM using Lookup tables

Figure 3.14 shows the response of the acceleration, speed and position of the rotor. The acceleration behaves the same way as the thrust does, with a maximum peak value of 22m/s at the initial stage. The speed starts at zero and then it traces a smooth path which increases gradually until it stabilizes at the steady state value around 12m/s, which was the value set as reference from the beginning. The position is traced by a smooth and progressive path which starts at 0m, reach 9m when the motor reaches the steady state after 2s the rotor has traveled around 16.2m. One can notice that the objective of implementing the Lookup tables was reached in which a rotor speed reference was enter as input to the system and the system returns the same value in the actual response.

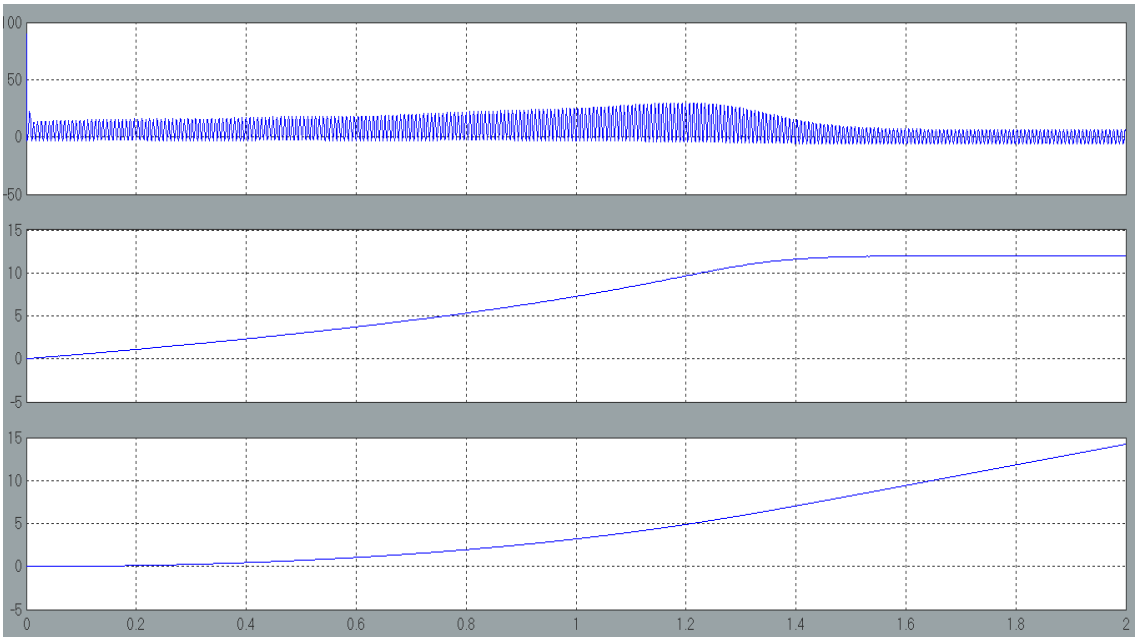

Figure 3.14: Acceleration, speed and position response of the rotor

Figure 3.15 shows the response of the mean thrust by varying the speed of the rotor. It can be notice once again a maximum peak value at the initial stage with a value 3733N which drops rapidly to 3142N and then starts to increase gradually until it reaches a maximum value around 5734N and then begin to decay quickly until it reaches and settle at 1640N, time at which the rotor speed has reached the steady state speed of 12m/s.

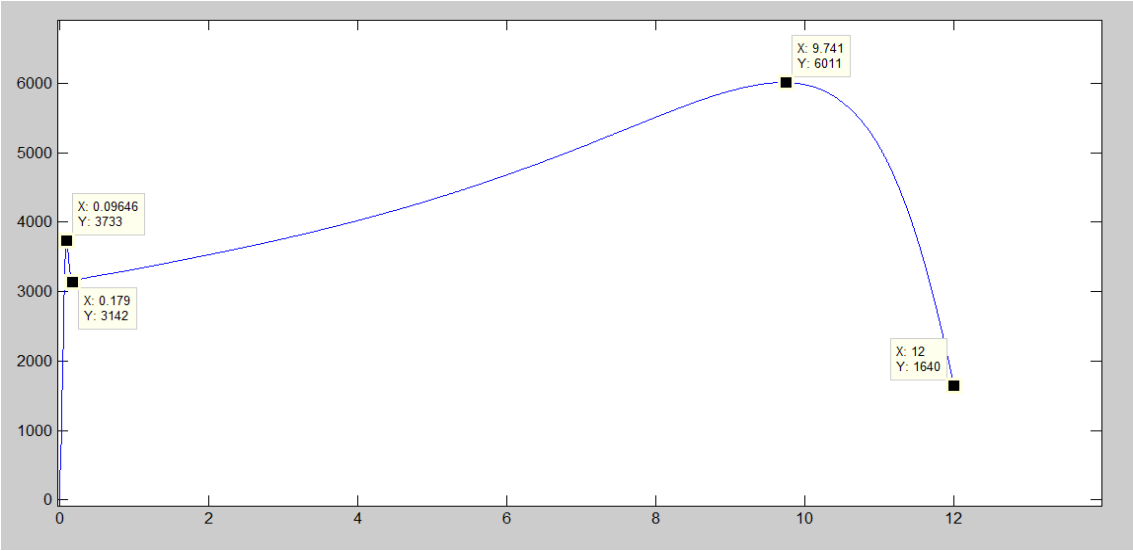

Figure 3.15: Mean Thrust versus v_r response of the LIM using Lookup tables

CHAPTER FOUR

AUTOMATIC CONTROL SYSTEM DESIGN FOR LIM

4.1 PID Controller

PID stands for Proportional-Integrative-Derivative which corresponds to the terms operating over the error signal in the controller [12]. The PID controller is the most widely used feedback controller m the industry. It calculates an error value as the difference between an actual (measured) signal and a reference value and then minimizes this error by adjusting the Input of the system. The PID controller is defined by the following equation:

$$u(t) = K_p e(t) + K_I \int e(t)d(t) + K_D \frac{d}{dt} e(t) \quad (4.1)$$

Where u(t) is the output of the PID Controller, $\boldsymbol{K_p}$, $\boldsymbol{K_I}$ and $\boldsymbol{K_D}$ are the proportional, integrative and derivative gains respectively and e(t) is the error signal define as:

$$e(t) = r(t) - y(t) \quad (4.2)$$

Where r(t) is the reference value and y(t) is the system output. By adjusting (tuning) the three gains, the controller can provide a good control action for a specific requirement, even with no knowledge of the process dynamics. The proportional term is the main gain. It makes a change to the value proportional to the current error value. A high proportional gain results in a large change in the output of the system for a certain change in the error and if it's too high can drive the system to instability.

The integral of the integrative term is the sum of the instantaneous errors over time and it gives the accumulated offset that should have been collected previously. The integral then multiplied by the integrative gain and added to the controller output, decreasing the rise time and eliminating the steady state error which cannot be accomplished only with the proportional term. However, if the gain is too high it can cause undesired overshoots. The derivative term is calculates the rate of change of the error in time and multiplies it by the derivative gain. It reduces the magnitude of the overshoot impart by the integrative term in exchange of slowing the transient response of the controller.

For this case of study, a PI controller was considered under the assumption that the inertia of the payload mass of the system will damp the response of the motor keeping simple the calibration of the controller. Thus, the response of the controller will be limited to only the first to terms of Equation (4.1). Figure 4.1, represents a conceptual diagram of the control system for this application, constituted mainly by the PI controller, the input voltage and the LIM. As can be seen, the PI Controller operates over the error signal, imparting the incremental of frequency necessary to lead the response of the motor to the reference value. The Lookup tables block is the one that sets the nominal frequency corresponding to the value of the speed reference.

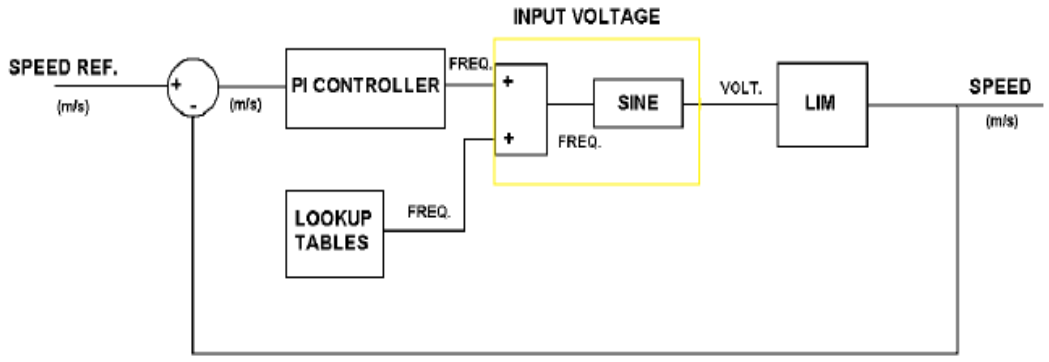

Figure 4.1: Conceptual diagram of the control system

4.2 LIM Speed Control.

On industrial applications different types of disturbances occur; on the sequel we will discuss two types of disturbances.

4.2.1 Case One

Figure 4.2shows MATLAB/SIMULINK model representing a disturbance force of 100% of the normal load with the value of 1000N and control using PI controller.

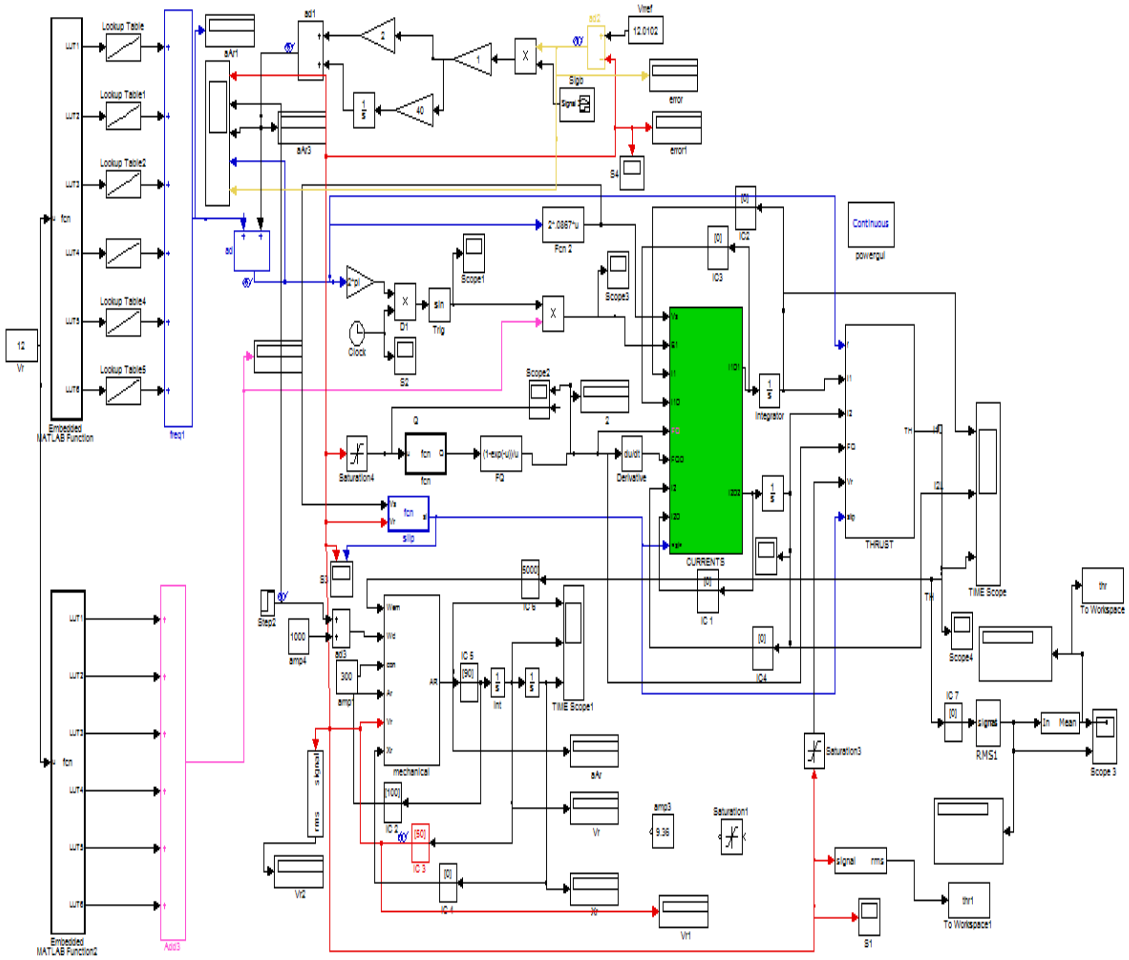

Figure 4.2: MATLAB/Simulink model of LIM using lookup tables and PI controller

For calibration of PI controller using manual tuning set $\boldsymbol{K_I}$ and $\boldsymbol{K_D}$ to zero,

and start changing $\boldsymbol{K_p}$ until the response of the system begins to oscillate, then $\boldsymbol{K_p}$ should be set to half of that value for a "quarter amplitude decay" type response. Then increase $\boldsymbol{K_I}$ until any offset is correct in sufficient time for the process. However, too much $\boldsymbol{K_I}$ will cause instability. Finally, increase$\boldsymbol{K_D}$, if required, until the loop is acceptably quick to reach its reference after a load disturbance. However, too much $\boldsymbol{K_D}$ will cause excessive response and overshoot.

Figure 4.2 shows the simulation model of LIM using lookup tables and PI controller

In the following analysis, a disturbing force of 100% of the normal load with a value of 1000N was added to the system at time 2s as one can see in Figure 4.3 on the second plot from top to bottom. One also can see from this Figure, that this adverse force led the system to diminish the rotor speed Vr from the reference value of 12m/s to 11.8m/s. The system remain this way until the PI controller is activated just at 2.5s, thus leading the system to reach ones again the reference rotor speed v_r in an interval of 0.2s (rise time) and settling after 0.4s (settling time), allowing to identify in Figure 4.4 four main zones in the response of the system: the Transient Zone, the Steady State, the Disturbance zone and finally the PI Activated Zone where v_r stabilizes in the reference value even though the disturbance and the PI response coexist.

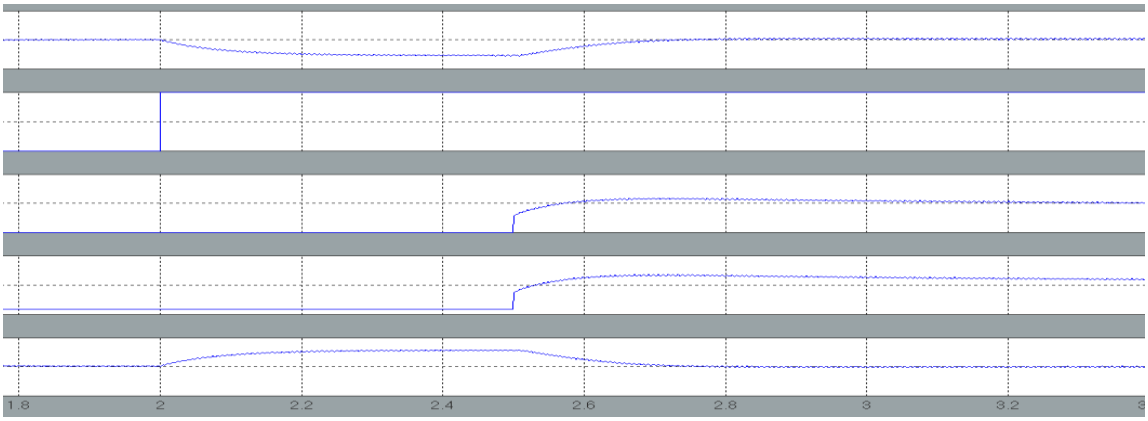

Figure 4.3: From top to bottom v_r $(zoomed)$, disturbance, PI response, frequency response and error

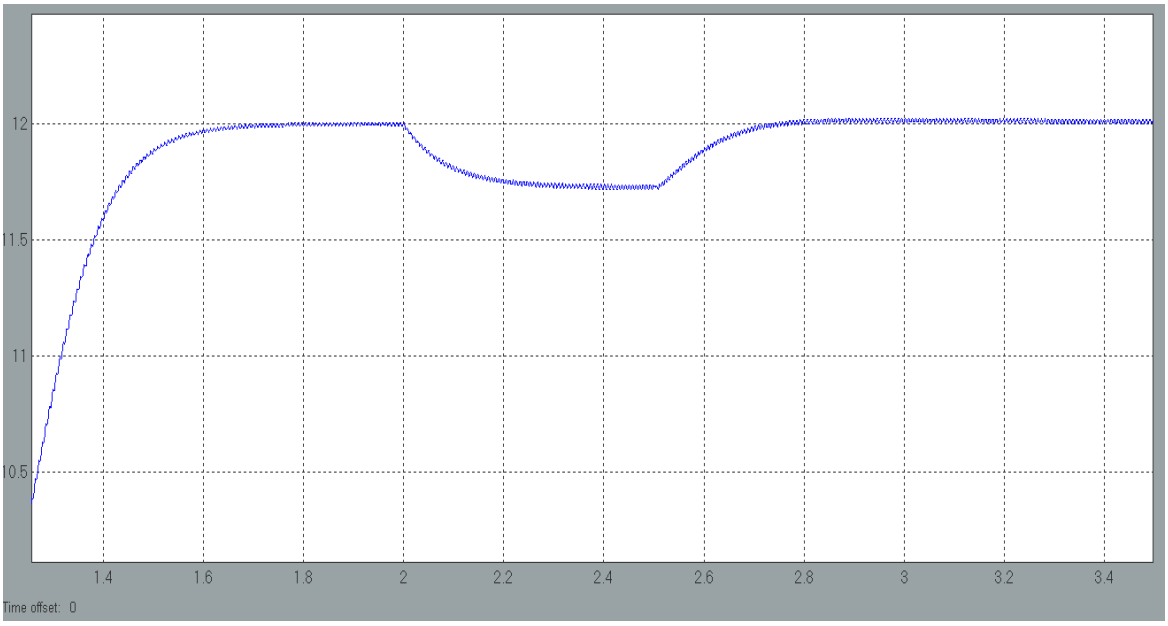

Figure 4.4: Rotor speed v_r $versus$ time

The simultaneously response of the PI controller are shown in detail on Figure 4.5 and Figure 4.6. One can see how the PI controller provide the system with an incremental of frequency with a maximum value of 1.18Hz at 2.7s and then drops rapidly until it stabilizes in a mean value of 1Hz. In Figure 4.7 one can see how the error comes from high values corresponding to the transient response of the system until it reaches the steady state and settles around zero. Then the disturbing force at 2s increase the error to a value of 0.28m/s and remains this way until the PI controller is activated at a time 2.5s settling the error signal again to zero after 0.4s.

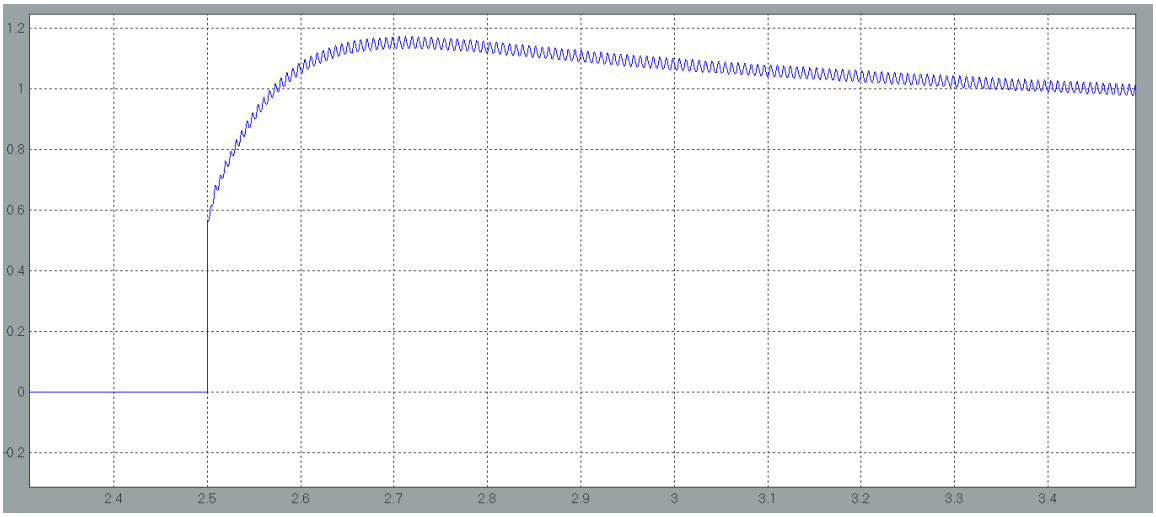

Figure 4.5: PI controller response

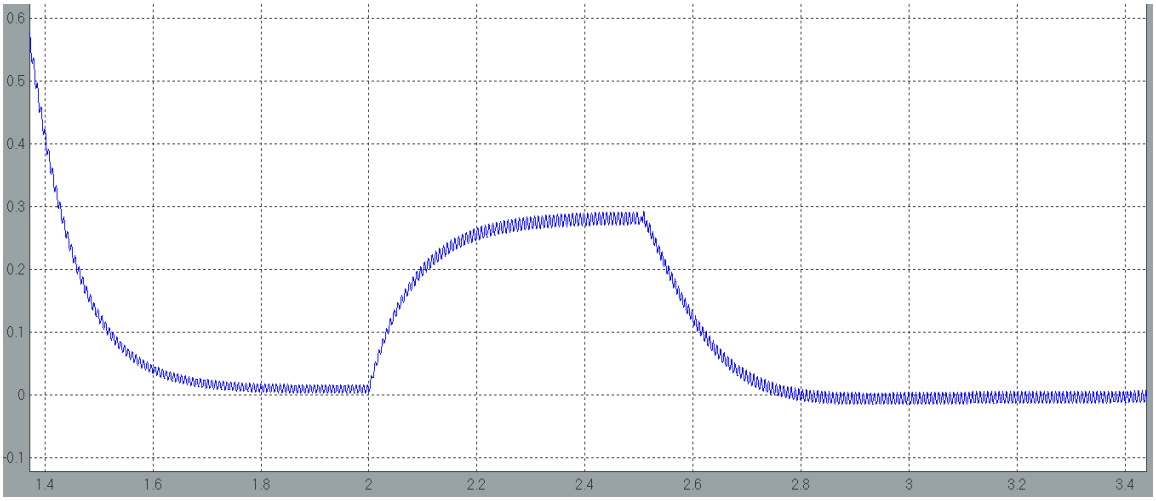

Figure 4.6: Error between reference speed and actual speed

Figure 4.7 shows the response of the rotor in terms of acceleration, speed and position. One can see how changes in the acceleration reflect the onset of the disturbing force and the PI response. One also can notice how the rotor has traveled around 32m after 3.5s over a smooth response path.

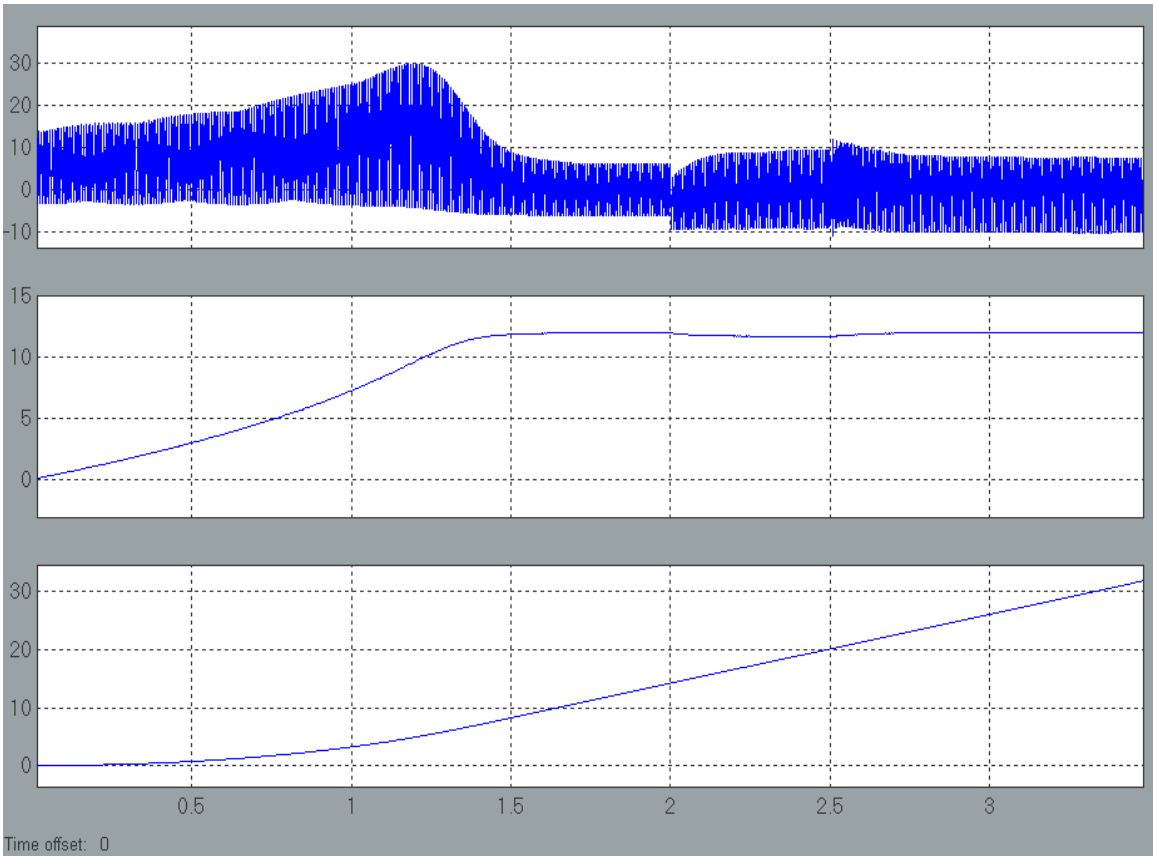

Figure 4.7: From top to bottom acceleration ,speed and position of rotor

Figure 4.8 also shows how the onset of the disturbance and the PI response affect the electric response of the system by trying to overcome these effects. For example one can notice how the rotor current is increased when the disturbance appears but then it decreases by the action of the PI controller. The stator current trace the same tendency in its response, however it increases its amplitude after the PI, provided that by increasing v_r, R_2/s will increase while R2f(Q) and Lm(l-f(Q)) will decrease in the per phase equivalent circuit, thus decreasing I2 but having a large increase in the magnetizing current (Im) and as a consequence an overall increase in the stator current I1.

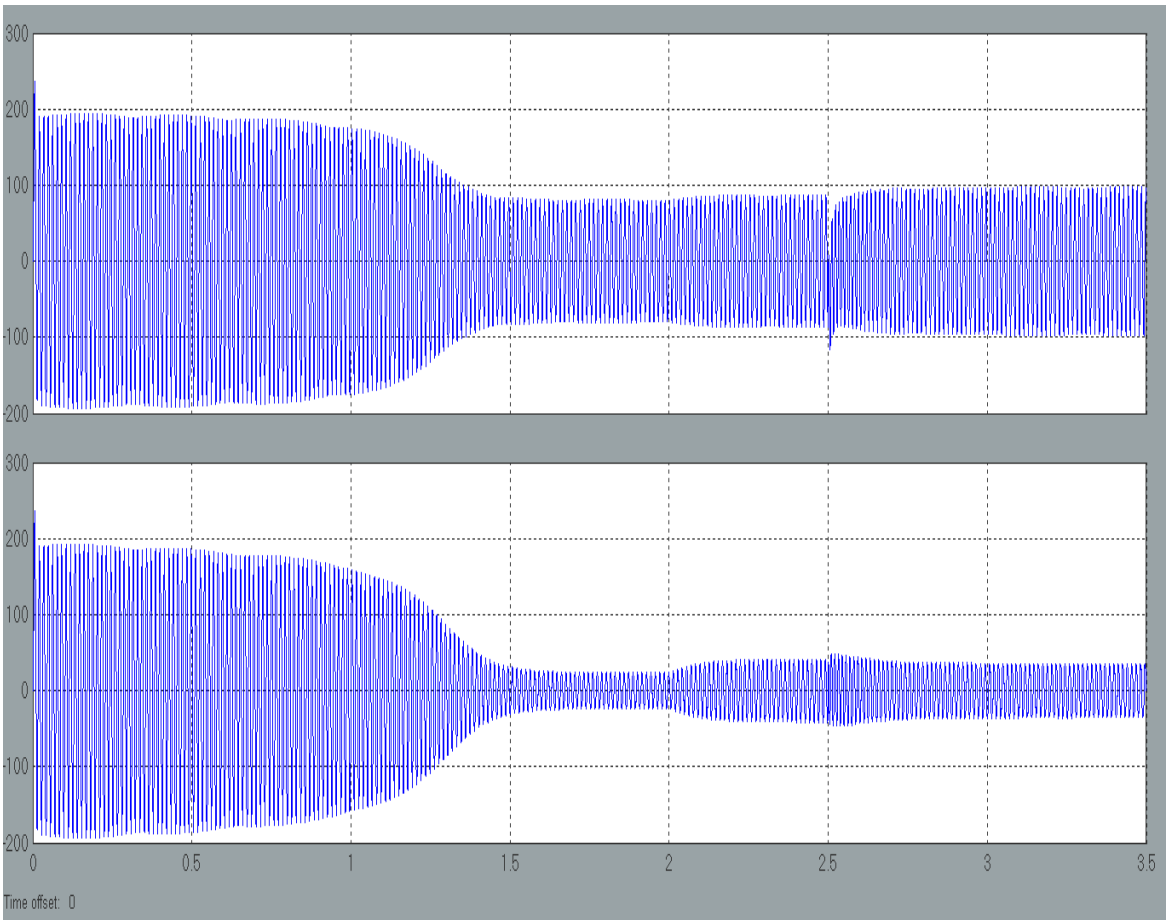

Figure 4.8: From top to bottom stator and rotor currents

4.2.2 Case Two

A disturbing force of 100% of the nominal load with a value of 1000N was added to the system at time 2s (similar to case one) as one can see in Figure4.9 and we will call this “Case two”. However the PI controller was also activated at the same time trying to overcome the effect of the disturbance immediately (unlike case one where the controller was activated after 5s of the disturbance presence), settling the rotor speed to the referenced value after 0.5s, as can be seen in Figure 4.10. Then, at a time of 3s , a change in the reference value of the rotor speed v_r take place. In terms of the simulation model, this means that the reference value of v_r changes for the input of the Lookup tables and also changes as the set value of the PI controller. Once the change on the set value is done, the Lookup tables change immediately the response to the new value of frequency, and if is necessary the second demultiplexer also will change the value of the voltage amplitude. Simultaneously, the PI controller is still activated and is absorbing all the possible instabilities this action causes. Finally, the system reaches the new speed reference after 0.5s and settles 0.6s later. The gains of the PI controller have changed to P=1 and I=60, once again by manual calibration, since different conditions are affecting the stability of the system.

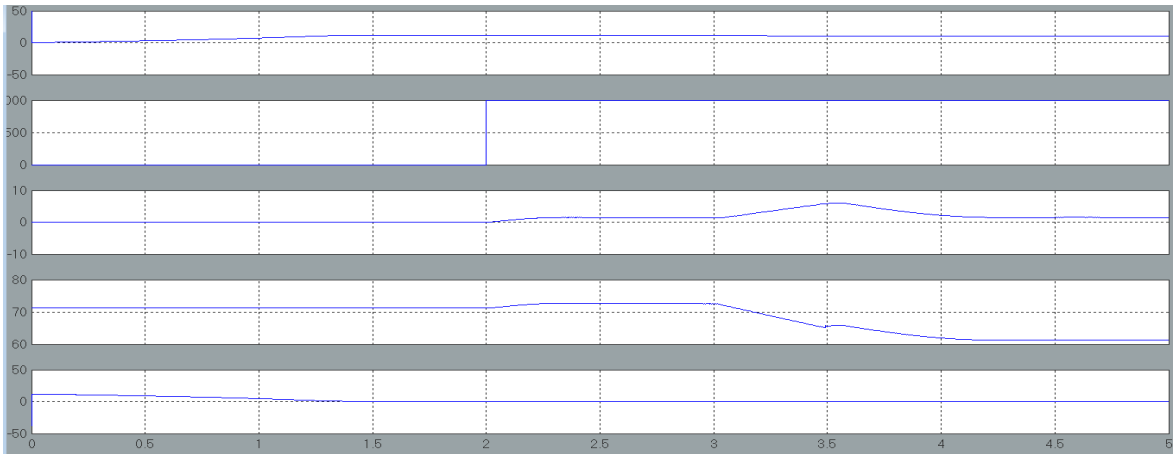

Figure 4.9: From top to bottom v_r,Disturbance, PI response, Frequency and Error for Case two

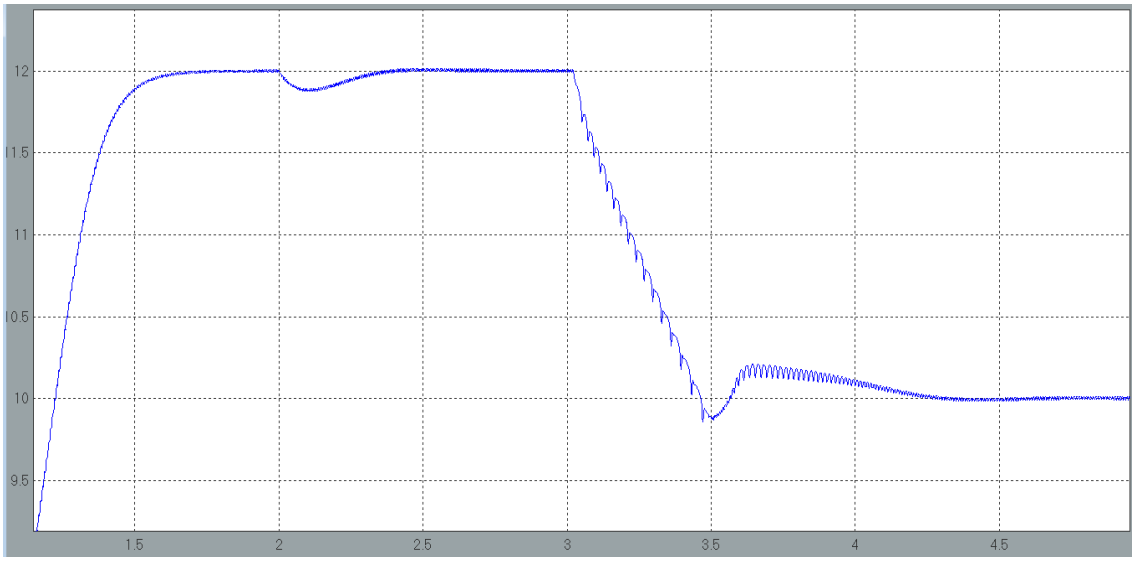

Figure 4.10: Rotor speed Vr (zoomed) for Case two

Figure 4.10, also shows the simultaneously response of the PI controller and the error, which are shown in detail on Figure 4.11 and Figure 4.12. One can see how the PI controller provide the system with the required frequency for each situation. At first it delivers a small value of frequency around 1.3Hz that leads the system to overcome the disturbance effects and reach the reference speed. Then, 1.3s later it increases rapidly to a higher value of frequency, about 6Hz that overcomes the effects of changing the reference speed. Ones it gets to the maximum value, it staffs to decrease gradually until some value around 1.45Hz. In Figure 4.12, one can see how the error comes from high values corresponding to the transient response of the system until it reaches the steady state and settles around zero. Then, the disturbing force at 2s increases the error to a maximum value of 0.12m/s. As the PI controller has been already activated, this small error drops and settles after 0.5s. Then, as the speed reference changed, the error increases rapidly to a maximum value of 0.25m/s and starts decreasing by action of the PI controller settling the error signal again to zero after 0.7s.

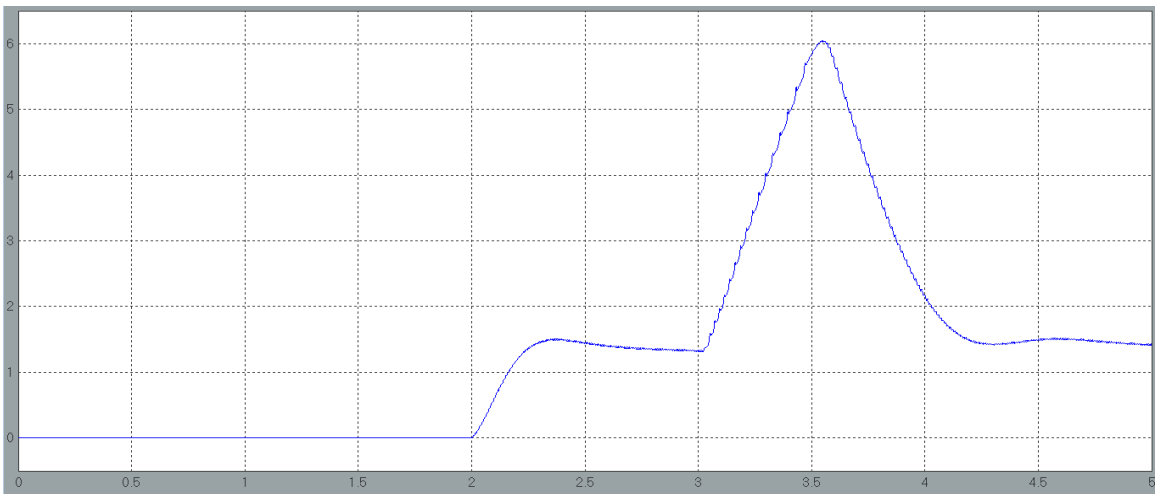

Figure 4.11: PI controller response for Case two

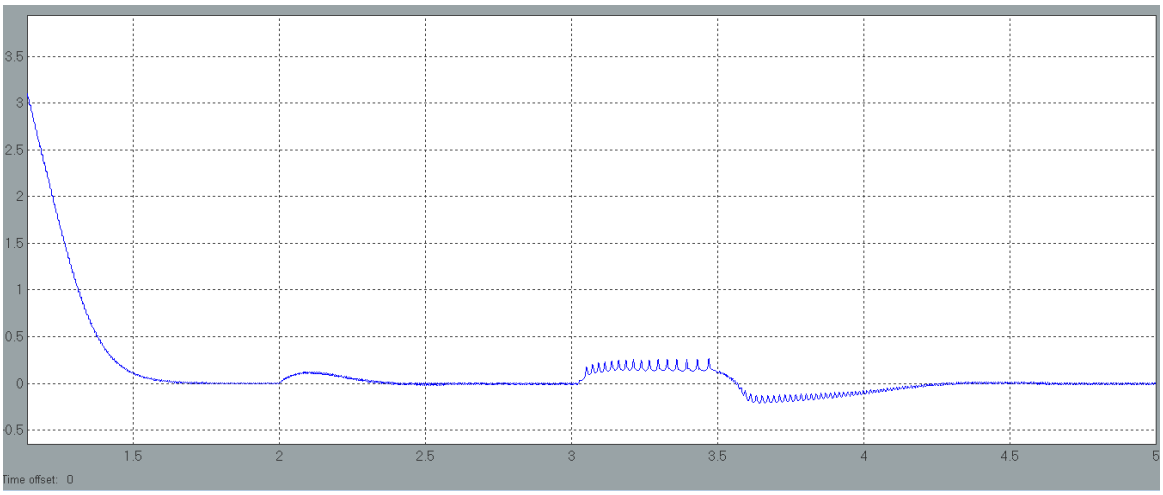

Figure 4.12: Error between the reference Vr and the output Vr for Case two

Figure 4.13, shows the response of the rotor in terms of acceleration, speed and position. One can see how changes in the acceleration reflect the onset of the disturbing force, the change in the speed reference and the PI response. One also can notice how the rotor has traveled around 47m after 5s over a smooth response.

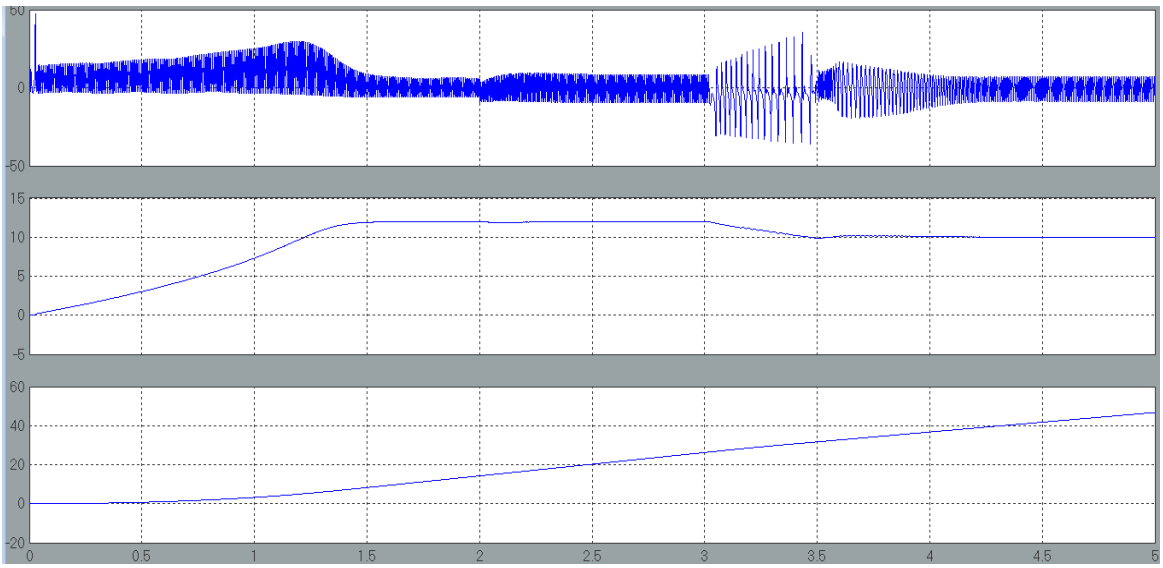

Figure 4.13: From top to bottom acceleration ,speed and position of rotor for Case two

Figure 4.14, also shows how the onset of the disturbance, the change of speed reference and the PI response, affect the electric response of the system by trying to overcome these effects. For example one can notice how the rotor current has a small increase when the disturbance appears simultaneously with the PI response and how it has a major increase due to the change of speed reference. The stator current trace the same tendency in its response. The increase in both currents due to the change of speed reference, can be explained as a decrease in Vr causes the slip (s) and R2/s to decrease, while R2f(Q) and increase, thus increasing the value of 12 and decreasing the magnetizing current (Im), resulting in an overall increase of the stator current I1. Refer to Figure 3.6 in chapter three which illustrate the per phase equivalent circuit for a LIM.

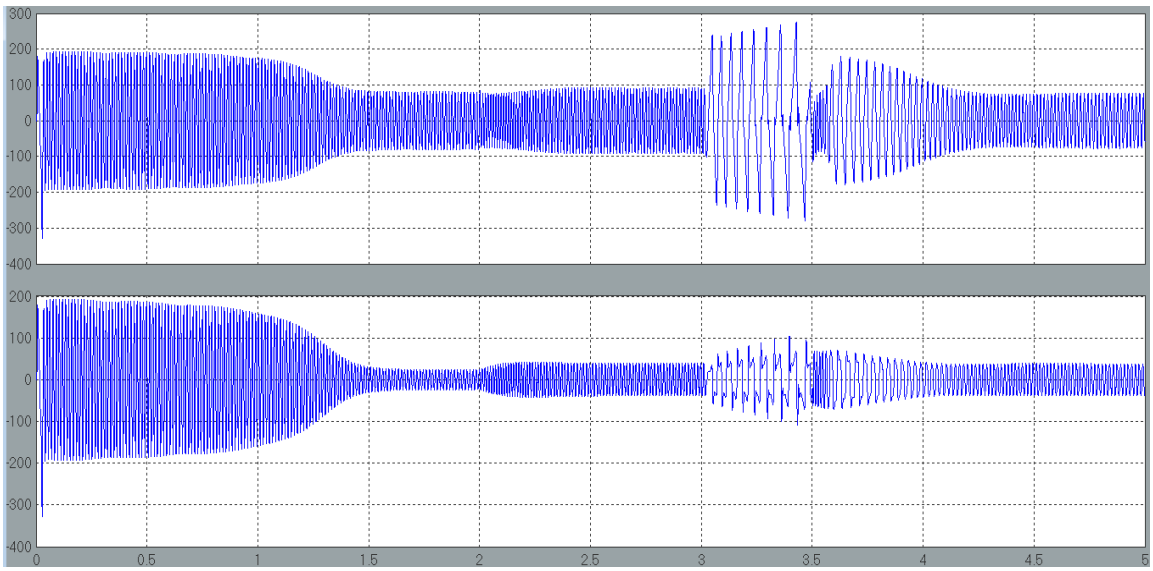

Figure 4.14: From top to bottom stator and rotor currents for case two

CHAPTER FIVE

CONCLUSION AND RECOMMENDATIONS

5.1 Conclusion

A functional simulation model based on the governing equations of the electromechanical system was developed and an evident similarity to the dynamic response of the RIM was observed, as one can see in the thrust Vs. Rotor speed plots (Figure 3.17) compared to the Torque Vs. Rotor speed of the RIM, in which is also distinguishable a starting value of thrust at the initial stage, after the initial transients have passed, a maximum value of thrust for a certain rotor speed value and from this point on, a progressive and fast decay of the thrust while the rotor speed keeps moving forward, until it finally reaches the synchronous speed where the value of thrust will be zero when no mechanical load is adopted, as no relative motion between the stator magnetic field and the secondary sheet is present.

The best way to cover a vast range of the rotor speed was found by defining an efficiency criterion at which the system would reach the steady state before certain time, which in this case was two seconds. This was developed as a first stage in the control of the LIM, where setting a desired speed of the rotor and reaching it rapidly were the main concerns. In order to achieve this compromise of reaching the reference speed in a small time, was found that the best way was not only by changing the frequency of the source but also the voltage amplitude. For that purpose two de-multiplexer blocks were implemented in the simulation model. The first one addressed the Lookup table corresponding to the range under which the speed reference of the rotor was covered outputting the optimum value of frequency. The second demultiplexer addressed the value of voltage amplitude corresponding to the speed reference of the rotor (upon defined ranges) necessary for the system to reach the desired conditions.

The most difficult part was on implementing the PI controller for which disturbing forces the controller, as the system is highly nonlinear and can lead to instability very easy. Also was found that the conventional tuning methods for the PI controller gains didn't work as expected, so manual calibration based on trial and error was the only way to get acceptable results for limited and specific conditions. This however could be overcome by implementing advance nonlinear control techniques which is suggested for further work

5.2 Recommendations

Future studies can use different methods for analysis of LIMs, such as Equivalent Circuit Model (ECM), 1-D and 2-D, electromagnetic field analysis and numerical methods including finite-element and finite-difference methods.

At this thesis manual tuning for PI controller is used but future studies can try different methods for the controller tuning .

A different type of controller also can be used in analysis may it gives better control characteristics

REFERENCES

[1] S. J. Chapman. *Electric Machinery Fundamentals*. New York: McGraw-Hill, 1985. pp. 152-162.

[2] M. Comanescu, L. Xu, "An Improved Flux Observer Based on PLL Frequency Estimator for Sensorless Vector Control of Induction Motors", IEEE Transactions on Industrial Electronics, Vol. 53, pp. 50-56, 2006.

[3] J. Duncan, "Linear Induction motor Equivalent Circuit Model", IEE Proceedings of Electric Power Applications B, Vol. 130, pp. 51-57, 1983.

[4] A.S. Gercek, V.M. Karsli," Performance Prediction of the Single-Sided Linear Induction Motors for Transportation Considers Longitudinal End Effect by Using Analytical Method", Contemporary Engineering science, Vol. 2, pp. 95-104, 2009.

[5] W. xu, J.G. Zhu, Y. Zhang, Z. Li, Y. Li, Y.Wang, Y. Guo,W. Li, "Equivalent Circuits for Single-Sided Linear Induction Motors ", IEEE Transactions on Industry Applications, Vol. 46, pp. 2410-2423, 2010.

[6] Abbas Shiri, Mohammad Reza AlizadehPahlavani, Abbas Shoulaie. "Secondary Back-Iron Saturation Effects on Thrust and Normal Force of Single-Sided Linear Induction Motor", Vol. 56 , pp. 110-119, 2012.

[7] E. R. Laithwaite and S. A. Nasar, "Linear-Motion Electrical Machines", Proceedings of the IEEE, Vol. 58, No. 4, 1970.

[8]Amir ZareBazghaleh, Mohammad Ren Naghashan, and Mohammad Reza Meshkatoddini, "Optimum Design of Single- Sided Linear Induction Motors for Improved Motor Performance" IEEE TRANSACTIONS ON transactions on magnetics, vol. 46, no. 1, 2010.

[9] Boucheta. ACOMPEL, "Adaptive Backstepping Controller for Linear Induction Motor Position Control", The International Journal for Computation and Mathematics in Electrical and Electronic Engineering, Vol.29, NO. 23, pp. 789-810, Emerald Croup Publishing Limited, 2010.

[10] A. Boucheta I. K. Bousserhane A. Hazzab P. Sicard and M. K. Fellah, "Speed Control of Linear Induction Motor using Sliding Mode Controller Considering the End Effects" Journal of Electrical Engineering and Technology, Vol. 7, No. 1, pp. 34-45, 2012.

[11]Mohammad Reza Satvati. Sadegh Vaez-Zadeh, "End-Effect Compensation in Linear Induction Motor Drives", 2010.

[12] Ang, K.H "PID Control System Analysis, Design, and Technology ", IEEE Transactions on Control Systems Technology, pp. 559-576, 2005.